International Journal of Nanomedicine

Dovepress
open access to scientific and medical research

Open Access Full Text Article

REVIEW

Nanotechnology-Based Drug Delivery Systems for Honokiol: Enhancing Therapeutic Potential and Overcoming Limitations

Jing Yang[1,2,*], Jinlu Shang[1,2,*], Liuxuan Yang[1,2,*], Daiqing Wei[3], Xia Wang[1], Qinmin Deng[2], Zhirong Zhong[4], Yun Ye[1], Meiling Zhou[1]

[1]Department of Pharmacy, The Affiliated Hospital of Southwest Medical University, Luzhou, Sichuan, People's Republic of China; [2]Department of Clinical Pharmacy, School of Pharmacy, Southwest Medical University, Luzhou, Sichuan, People's Republic of China; [3]Department of Orthopaedics, The Affiliated Hospital of Southwest Medical University, Luzhou, Sichuan, People's Republic of China; [4]Department of Pharmaceutical Sciences, School of Pharmacy, Southwest Medical University, Luzhou, Sichuan, People's Republic of China

*These authors contributed equally to this work

Correspondence: Meiling Zhou, Email meilzhou@163.com

Abstract: Honokiol (HNK) is a small-molecule polyphenol that has garnered considerable attention due to its diverse pharmacological properties, including antitumor, anti-inflammatory, anti-bacterial, and anti-obesity effects. However, its clinical application is restricted by challenges such as low solubility, poor bioavailability, and rapid metabolism. To overcome these limitations, researchers have developed a variety of nano-formulations for HNK delivery. These nano-formulations offer advantages such as enhanced solubility, improved bioavailability, extended circulation time, and targeted drug delivery. However, existing reviews of HNK primarily focus on its clinical and pharmacological features, leaving a gap in the comprehensive evaluation of HNK delivery systems based on nanotechnology. This paper aims to bridge this gap by comprehensively reviewing different types of nanomaterials used for HNK delivery over the past 15 years. These materials encompass vesicle delivery systems, nanoparticles, polymer micelles, nanogels, and various other nanocarriers. The paper details various HNK nano-delivery strategies and summarizes their latest applications, development prospects, and future challenges. To compile this review, we conducted an extensive search using keywords such as "honokiol", "nanotechnology", and "drug delivery system" on reputable databases, including PubMed, Scopus, and Web of Science, covering the period from 2008 to 2023. Through this search, we identified and selected approximately 90 articles that met our specific criteria.

Keywords: honokiol, nanotechnology, drug delivery, targeting, antitumor, bioavailability

Introduction

Honokiol (HNK) is a hydrophobic polyphenolic compound extracted from Magnolia officinalis. Preclinical studies have demonstrated that HNK does not exhibit mutagenic or genotoxic effects in vitro and in vivo.[1,2] Moreover, it possesses various physiological effects, including anticancer,[3] anti-oxidative stress,[4] anti-inflammatory,[5] anti-bacterial,[6] anti-viral,[7] anti-obesity,[8] anti-diabetes,[9] and anti-fibrosis activities.[10] These remarkable characteristics make HNK a promising candidate for the development of novel therapeutic agents.

HNK exhibits effective blood-brain barrier penetration, exerting neuroprotective effects by promoting cell growth.[11] Additionally, it displays anti-diabetic and anti-obesity effects by enhancing insulin sensitivity and promoting white adipose tissue browning.[12,13] HNK also exerts antibacterial properties by inducing apoptosis and inhibiting biofilm formation.[14] The antitumor effects of HNK have attracted significant research attention, given its capacity to induce G0/G1 and G2/M cell cycle arrest, inhibit cell migration and invasion, anti-angiogenesis, and suppress the expression of Forkhead Box M1.[15,16] Moreover, HNK can reduce the expression of P-glycoprotein (P-gp), suppress oxidative stress, and inhibit pro-inflammatory cytokines such as IL-6, IL-1β, and THF-α.[14] Notably, a phase I clinical trial of liposome-

Received: 27 July 2023
Accepted: 30 October 2023
Published: 13 November 2023

Graphical Abstract

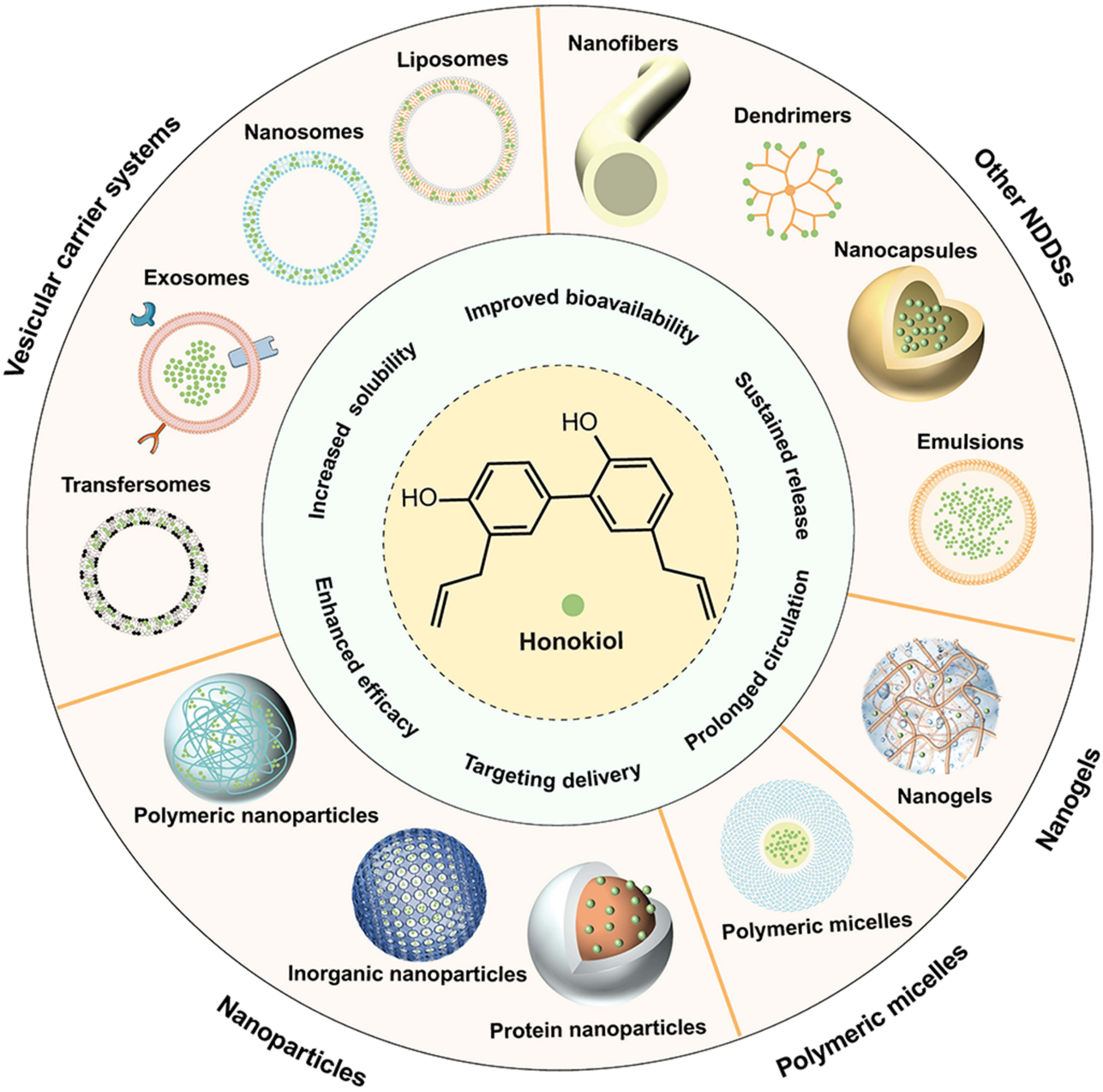

encapsulated HNK in advanced non-small cell lung cancer (NSCLC) patients (CTR20170822) is currently underway in China.[17] However, the clinical utilization of HNK is hindered by its poor solubility, low bioavailability, instability, and fast metabolism.[3,18] Previous studies have reported that the oral bioavailability of HNK is only about 5% owing to its extensive first-pass metabolism and poor absorption.[19] Consequently, it is imperative to explore novel strategies to overcome these disadvantages of HNK.

In recent years, nanotechnology-based drug delivery systems (NDDSs) have received extensive attention for their promising applications in disease diagnosis, monitoring, and treatment. Various methods are available to prepare NDDSs, with green synthesis standing out as a high-yield, low-toxicity, stable, cost-effective, and environmentally friendly

approach that can endow NDDSs with excellent safety profiles.[20–22] In addition, NDDSs hold the potential to enhance the solubility, stability, and bioavailability of drugs by optimizing the physical and chemical properties of the nanocarrier.[23] For instance, the utilization of stimuli-responsive materials in nanocarriers allows for smart drug release in specific microenvironments.[24] Additionally, nano-formulations can effectively enhance drug permeability and retention in tumor tissues, resulting in passive targeting effect.[25] Furthermore, specific ligands can be employed to modify NDDSs to achieve active targeting ability for improving therapeutic efficacy while reducing side effects.[26] Based on this, researchers have successfully encapsulated HNK within various nanocarriers, such as liposomes,[27] nanoparticles,[28] polymer micelles,[29] nanogels,[30] self-microemulsion delivery systems,[31] and dendrimers.[32] Moreover, researchers have explored the co-delivery of HNK with other chemotherapeutic agents or the utilization of photothermal materials to achieve synergistic effects from multiple therapies.[28,33] These NDDSs have endowed HNK with improved solubility, enhanced bioavailability, targeting activity, prolonged circulation time, and slowed metabolism, ultimately leading to enhanced therapeutic efficacy.

To date, a systematic review of HNK-loaded nano-formulations has not been reported. Therefore, this paper aims to provide a comprehensive overview and summary of NDDSs developed for HNK and offer novel insights for the application of natural compounds.

Vesicular Carrier Systems

Vesicles are supramolecular aggregates that result from the self-assembly of amphiphilic molecules, forming spherical structures with single or multiple chambers enclosed by a bilayer membrane. The bilayer membrane of vesicles allows for the encapsulation of hydrophobic drugs, while the aqueous center can dissolve hydrophilic drugs, thus enabling the simultaneous encapsulation of both hydrophilic and lipophilic molecules. Vesicles offer advantages such as biodegradability, increased solubility, prolonged blood circulation time, and improved bioavailability,[34] which have gained increasing attention in the field of biomedicine. Several vesicular carrier systems have been employed for the delivery of HNK, including liposomes, nanosomes, exosomes, and transfersomes, as summarized in Table 1.

Liposomes

Liposomes refer to amphiphilic spherical vesicles composed of phospholipids and cholesterol with a lipid bilayer structure, which can be prepared by thin film hydration, reverse evaporation, or ethanol injection methods.[55] Chen's group has performed several studies on PEGylated HNK liposomes,[35–39] demonstrating enhanced solubility, increased plasma drug concentration, and prolonged half-life. In one study, HNK liposomes were prepared for the treatment of gefitinib-sensitive (HCC827) and gefitinib-resistant (H1975) NSCLC.[36] Significant antitumor effects were observed in both HCC827 and H1975 xenograft mouse models treated with HNK liposomes at various doses. Additionally, they proposed an approach to improve encapsulation efficiency and stability by entrapping inclusion complexes within liposomes.[37] This method involved initially binding HNK to HP-β-CD and subsequently encapsulating it in liposomes, resulting in an average size of 123.5 nm and encapsulation efficiency of 91.09 ± 2.76%. These liposomes demonstrated delayed drug release characteristics and prolonged circulation time. Moreover, Li et al developed HNK liposomes for glioma therapy, demonstrating the ability to inhibit tumor growth by up-regulating M1 macrophages while down-regulating M2 macrophages simultaneously.[56]

Single-agent chemotherapy often fails to achieve satisfactory efficacy or may lead to drug resistance. Therefore, combining or co-delivering HNK with other drugs has emerged as a promising strategy to enhance treatment outcomes. For instance, a study on ovarian cancer demonstrated that the combination of HNK liposomes with DDP achieved a remarkable tumor inhibition rate of 91.48%, whereas the inhibition rates of HNK liposomes and DDP alone were only 66.83% and 52.5%, respectively.[41] Similarly, Jiang and Cheng et al reported enhanced antitumor effects by combining HNK liposomes with DDP in lung and colon cancer treatments.[42,43] Another study investigated the combination of HNK liposomes with DOX for breast cancer treatment.[44] After 26 days of administration, a significant reduction in tumor volume was observed in the combined treatment group (150.62 ± 36.42 mm^3) compared to those treated solely with either HNK liposomes (605.98 ± 121.51 mm^3) or DOX (539.99 ± 128.29 mm^3). Furthermore, Jin et al prepared a cocktail liposome system to co-deliver HNK, ginsenoside Rh2, betulinic acid, parthenolide, and HNK to enhance the therapeutic

Table 1 Summary of HNK-Loaded Vesicular Carrier Systems

Type	Materials/Combined Therapy	Preparation Methods	Physicochemical Properties	Cells	Animal Models	Main Effects	Ref.
Liposomes	Phosphatidylcholine, cholesterol, $MPEG_{2000}$-DSPE	Thin-film dispersion method	PS: 98.68 nm; ZP: −20.6 mV; EE: ~87.68%	NA	NA	Increased solubility; improved pharmacokinetics	[35]
	SPC, cholesterol, PEG_{2000}-DSPE	Thin-film dispersion method	PS: ~130 nm; ZP: −20.0 to −30.0 mV; EE: 85%; DL: 14.6%	HCC827; H1975; H460; SPC-A1; H441; H1650; H226; H522; H1993	H1975, HCC827, H460 and SPC-A1 xenograft tumor-bearing mice	Promoted degradation of heat shock protein 90 client protein; enhanced antitumor activity	[36]
	HP-β-CD, SPC, cholesterol, $MPEG_{2000}$-DSPE, vitamin E	Ethanol injection method	PS: 123.5 nm; ZP: −25.6 mV; EE: ~91.09%	A549; HepG2	NA	Sustained drug release; prolonged blood circulation	[37]
	PC, cholesterol, PEG4000	Thin-film dispersion method	PS: ~150 nm	A2780s; A2780cp	A2780s and A2780cp xenograft tumor-bearing mice	Enhanced antitumor effect; prolonged survival time	[38]
	PC, cholesterol, PEG4000	Thin-film dispersion method	PS: ~130 nm	VEGF-D-LL/2	High-expression VEGF-D-LL/2 tumor-bearing mice	Inhibited tumor-associated lymphangiogenesis and metastasis; slowed tumor growth; prolonged life span	[39]
	Lipoid E80, Kolliphor HS15	Thin-film dispersion method	PS: ~80.62 nm; ZP: ~ −3.91 mV; EE: ~92.4%; DL: ~6.7%	LLC	LLC tumor-bearing mice	Enhanced bioavailability and antitumor effect; increased tumor accumulation	[40]
	Lecithin, PEG4000, cholesterol (co-treatment: DDP)	Thin-film dispersion method	PS: ~130 nm	SKOV3	SKOV3 xenograft tumor-bearing mice	Synergistic antitumor effect	[41]
	PEG4000-PE, cholesterol, PC (co-treatment: DDP)	Thin-film dispersion method	PS: ~150 nm	A549	A549 xenograft tumor-bearing mice	Synergistic antitumor effect; prolonged life span	[42]
	Cholesterol, PEG4000 (co-treatment: DDP)	Thin-film dispersion method	PS: ~120 nm	CT26	CT26 tumor-bearing mice	Increased solubility; synergistic antitumor effect	[43]
	Cholesterol, PEG4000 (co-treatment: DOX)	Thin-film dispersion method	PS: ~150 nm	4T1	4T1 tumor-bearing mice	Improved solubility; synergistic antitumor effect	[44]
	Phosphatidylcholine, DSPE-PEG2000, cholesterol (co-delivery: ginsenoside Rh2, parthenolide, betulinic acid)	Thin-film dispersion method	PS: 115.7 nm; ZP: −18.31 mV; EE: 91.4%	A549	A549 xenograft tumor-bearing mice	Synergistic antitumor effect	[45]

Targeting liposomes	EPC, DOPE, DOTAP, Cholesterol (targeting moiety: HA)	Thin-film dispersion method	PS: ~162.6 nm; ZP: −38.24 mV; EE: 89.3–92.5%	4T1	4T1 tumor-bearing mice	Higher tumor accumulation; improved antitumor and anti-metastasis effect	[46]
	SPC, cholesterol, DSPE-mPEG2000 (targeting moiety: HA)	Thin-film dispersion method	PS: ~146.20 nm; ZP: ~ −38.45 mV; EE: ~80.14%; DL: ~3.78%	143B; MCF-7 cell	143B xenograft tumor-bearing mice	Tumor targeting; enhanced antitumor activity	[47]
	EPC, DOPE, DOTAP, cholesterol (targeting moiety: PSA)	Thin-film dispersion method	PS: ~184.2 nm	4T1	4T1 tumor-bearing mice	Tumor targeting; enhanced antitumor and anti-metastasis efficacy	[48]
	^{D}CDX-PEG$_{2000}$-DSPE, SPC, DSPE-PEG$_{2000}$, cholesterol, (co-delivery: DSF/Cu; targeting moiety: ^{D}CDX peptide)	Thin-film dispersion method	PS: 122.5 nm; ZP: 1.36 mV; EE: ~87.8%; DL: ~3.25%	U87; C6; bEnd.3	Orthotopic U87 and C6 tumor-bearing mice	Tumor targeting; remodeled tumor immune microenvironment; extended survival time; synergistic antitumor effect	[27]
	EPC, cholesterol, DSPE-PEG$_{2000}$, DSPE-PEG$_{2000}$-NHS (co-delivery: daunorubicin; targeting moiety: Lf)	Thin-film dispersion method and ammonium sulfate gradient methods	PS: ~104.14 nm; ZP: ~4.15 mV; EE: ~96.90%	C6; BMVECs	C6 tumor-bearing mice	Higher tumor accumulation; synergistic antitumor effect; extended survival time	[49]
	EPC, cholesterol, DSPE-PEG$_{2000}$, DSPE-PEG$_{2000}$- OCT (co-delivery: epirubicin; targeting moiety: OCT)	Thin-film hydration method and ammonium sulfate gradient methods	PS: ~108.22 nm; ZP: ~ −3.23 mV; EE: ~96.41%	LLT	LLT tumor-bearing mice	Selective tumor accumulation; synergistic antitumor effect; prolonged survival time	[50]
	EPC, cholesterol, DC-cholesterol, DSPE-PEG$_{2000}$ (co-delivery: daunorubicin; targeting moiety: HA)	Thin-film hydration method and ammonium sulfate gradient methods	PS: ~112.65 nm; ZP: ~3.23 mV; EE: ~96.66%	MCF-7; MDA-MB-435S	MDA-MB-435S xenograft tumor-bearing female mice	Increased circulation time; selective tumor accumulation; synergistic antitumor effect; destroyed VM channels	[51]
Nanosomes	Soybean phosphatidylcholine, cholesterol	Ultra-high pressure homogenization method	PS: ~48.0 nm; EE: ~58.1%	NA	Autoimmune encephalomyelitis mice	Ameliorated encephalomyelitis; reduced demyelination and inflammation	[52]
Exosomes	Mesenchymal stem cells	Sonication method	PS: ~175.3 nm; ZP: ~12.9 mV; EE: ~80%	MiaPaCa; Colo357; MDA-MB-231; HT-29; LNCaP; SKOV3	NA	Enhanced intracellular accumulation and antitumor efficiency	[53]
Transfersomes	Lecithin, sodium deoxycholate, glycerol	Modified scalable heating method	PS: ~189.9 nm; ZP: ~ −53.4 mV; EE: ~78.92%	B16F10; RAW246.7; L929	NA	Alleviated stem-like cell characteristics and immunosuppression of melanoma cells	[54]

Abbreviations: PEG4000, polyethylene glycol 4000; DDP, cisplatin; PS, particle size; PC, phosphatidyl cholines; DOX, doxorubicin; PE, phosphoethanolamine; VEGF-D, vascular endothelial growth factor D; MPEG$_{2000}$-DSPE, methoxy (polyethylene glycol)-2000-distearoyl phosphatidylethanolamine; ZP, zeta potential; EE, encapsulation efficiency; NA, not available; HP-β-CD, hydroxypropyl-β-cyclodextrin; SPC, soybean lecithin; DL, drug loading; EPC, egg yolk phosphatidylcholine; NHS, N-Hydroxy succinimide; Lf, lactoferrin; OCT, octreotide; HA, hyaluronic acid; DOPE, dioleoyl phosphoethanolamine; DOTAP, 1,2-dioleoyl-3-trimethylammonium-propane (chloride salt); DSF/Cu, disulfiram/copper; PSA, polysialic acid; VM, vasculogenic mimicry.

https://doi.org/10.2147/IJN.S431409

efficiency against lung cancer while mitigating drug resistance issues simultaneously.[45] The apoptosis rates of cells treated with HNK, ginsenoside Rh2, betulinic acid, and parthenolide were found to be 30.4%, 21.6%, 31.1%, and 35.6%, respectively. However, the cocktail liposome group induced a significantly higher cell apoptosis rate of 63.6% than the single drug groups. In addition, Li et al combined HNK liposomes with the autophagy inhibitor chloroquine, which effectively inhibited the growth of medulloblastoma.[57] Although the combination therapy exhibited promising synergistic effects, the underlying mechanisms require further elucidation. Additionally, careful consideration should be given to the optimal drug ratio for combination therapy to maximize treatment benefits.

Despite the enhanced therapeutic efficacy of HNK liposomes, the limited targeting ability greatly restricts their potential applications.[58] To address this challenge, Wang et al reported HA-modified HNK cationic liposomes (HA-Lip-HNK) for anti-breast cancer and anti-tumor metastasis.[46] The results showed that the signal intensity of the DiR-labeled HA-Lip-DiR group continuously increased up to 6 hours and remained visible at 24 hours. In contrast, only a slight fluorescent signal was detected at the tumor site in the unmodified liposomes, proving the enhanced tumor-targeting capability of HA-Lip-DiR. Moreover, in the 4T1/Luc (luciferase-labeled) breast cancer lung metastasis model, the HA-Lip-HNK group exhibited the lowest bioluminescent intensity and the most potent anti-metastasis capacity compared to the HNK and Lip-HNK groups. A study by Zhang et al developed an HNK-loaded liposome modified with HA-phospholipid conjugate (HA-DOPE@Lips/HNK), which enhanced the targeting ability via interactions between HA and CD44 receptors highly expressed on tumor cells.[47] Both in vivo and in vitro studies demonstrated that HA-DOPE@Lips/HNK specifically delivered HNK to tumor cells and exerted significant anti-osteosarcoma effects. Li et al also prepared PSA-modified HNK-loaded cationic liposomes, which facilitated cellular uptake and cytotoxicity through PSA-selectin receptor-mediated endocytosis.[48] This formulation markedly inhibited tumor growth and metastasis in 4T1 tumor-bearing mice.

In another research, Zheng et al developed ^{D}CDX peptide-modified brain-targeted liposomes (CDX-LIPO) that co-delivered HNK and DSF/Cu to remodel the tumor immune microenvironment.[27] CDX-LIPO effectively inhibited the growth of malignant glioma by targeting the mammalian target of rapamycin pathway, inducing autophagy and immunogenic cell death, as well as regulating tumor metabolism and microenvironment. Figure 1A and B demonstrate the wide distribution of CDX-LIPO at tumor sites with minimal detection in normal brain tissue, whereas the unmodified liposomes (LIPO) exhibited weak fluorescence within the glioma area. This indicated that ^{D}CDX modification facilitated liposome penetration across the blood-brain barrier and enhanced their targeting efficacy in the glioma microenvironment. In the in vivo experiment, the CDX-LIPO group displayed a median survival time of 27 days, compared to 21 days in both the free drug combination group and LIPO group (Figure 1C). Notably, 30% of mice treated with CDX-LIPO were still alive at the end of the experiment, indicating a significant enhancement in antitumor activity. Additionally, Li's group conducted several studies on liposomes for targeted delivery of HNK.[49–51] They designed Lf-modified daunorubicin and HNK co-delivered liposomes for treating glioma,[49] OCT-modified epirubicin and HNK co-loaded liposomes for the treatment of NSCLC,[50] and HA-modified daunorubicin and HNK co-delivered liposomes for breast cancer therapy.[51] Notably, all of these liposomal formulations exhibited remarkable antitumor effects. However, the challenge of improving the drug loading rate remains an aspect that requires further attention.

Nanosomes

Extrusion and ultrasound are commonly employed techniques for the preparation of liposomes. However, achieving liposomes with a particle size below 100 nm remains challenging, accompanied by limited reproducibility. To overcome these limitations, the high-pressure homogenization method has emerged as a viable solution, enabling the manufacturing of liposomes with a narrow size distribution and particle sizes ranging from 20 to 50 nm, which are commonly referred to as nanosomes.[59] Hsiao et al successfully prepared an HNK-loaded nanosome (NHNK) characterized by a high drug loading capacity (58.1 ± 4.2%) and a uniform nanometer size (48.0 ± 0.1 nm).[52] Notably, NHNK demonstrated the ability to alleviate the severity of experimental autoimmune encephalomyelitis by inhibiting the infiltration of activated Th1 and microglia cells into the spinal cord. In addition, investigations revealed that HNK-loaded nanosomes were effective in ameliorating DDP-induced chronic kidney injury and testicular injury,[60,61] thereby improving the clinical safety of DDP in cancer treatment.

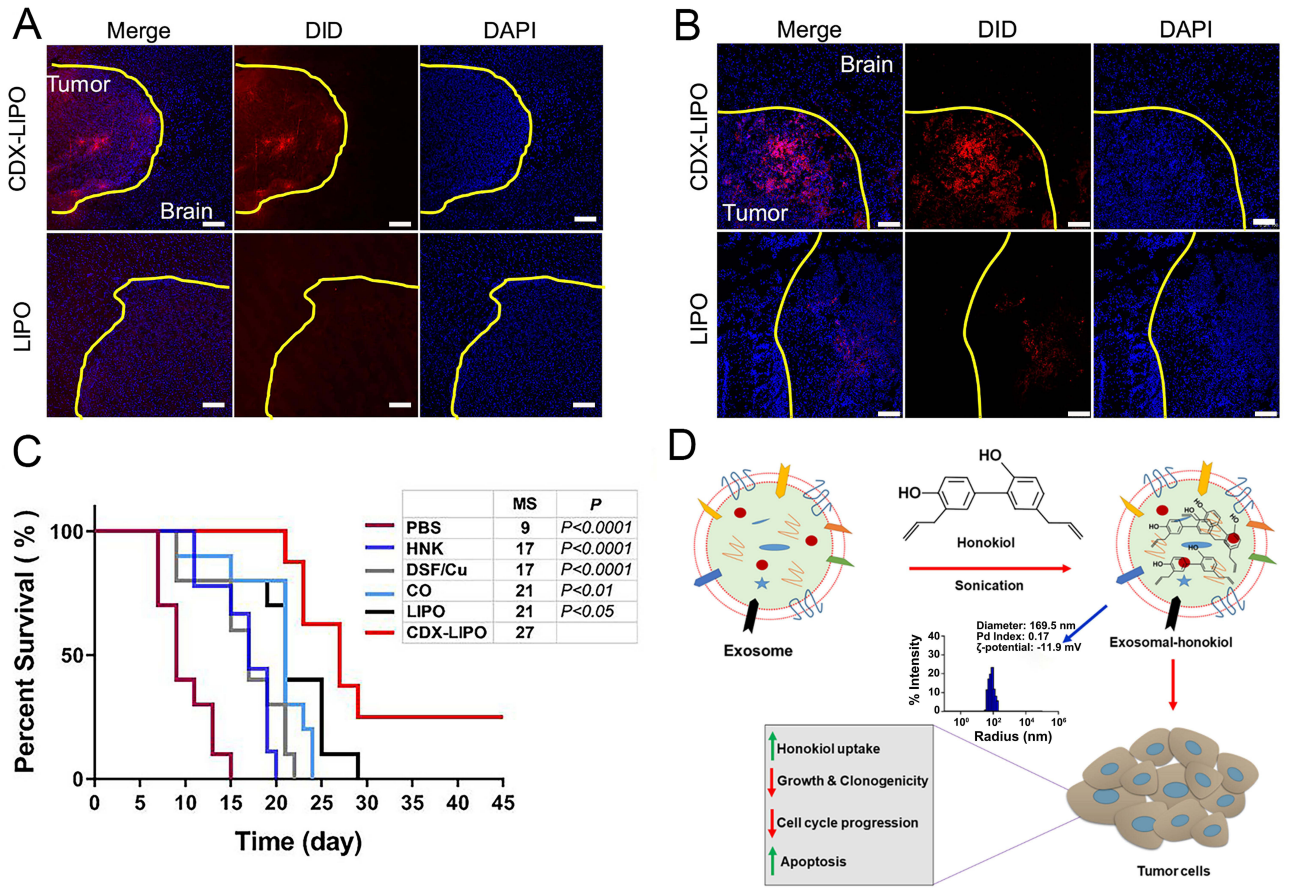

Figure 1 Immunofluorescence images of brain slices from (**A**) nude mice and (**B**) Balb/c mice (scale bar: 100 μm). (**C**) Survival curves of C6 orthotopic glioma mouse model. The italic font *P*<0.0001, *P*<0.01, and *P*<0.05 indicate the statistical significance of the CDX-LIPO group compared to other groups. CO: free drug combination group. Reprinted from Zheng Z, Zhang J, Jiang J, et al. Remodeling tumor immune microenvironment (TIME) for glioma therapy using multi-targeting liposomal codelivery. *J Immunother Cancer*. 2020;8(2):e000207. Creative Commons.[27] (**D**) Schematic diagram illustrating the mechanism of HNK-loaded exosomes. Reprinted from Kanchanapally R, Khan MA, Deshmukh SK, et al. Exosomal formulation escalates cellular uptake of honokiol leading to the enhancement of its antitumor efficacy. *Acs Omega*. 2020;5 (36):23299–23307. Copyright © 2020 American Chemical Society. Creative Commons.[53]

Exosomes

Exosomes, extracellular vesicles formed through the fusion and exocytosis of intracellular multivesicular bodies with plasma membranes, possess a lipid bilayer structure with a diameter of approximately 40–160 nm.[62] Owing to their natural transport capabilities, exosomes exhibited reduced toxicity and higher biocompatibility, making them suitable for repeated administration.[63] In the context of HNK delivery, mesenchymal stem cell-derived exosomes were utilized to prepare HNK-loaded nano-formulations, referred to as Exo-HK (Figure 1D), with an average size of approximately 175.3 nm.[53] Compared with free HNK, the uptake of Exo-HK by MiaPaCa and Colo357 pancreatic cancer cells was significantly increased by 3.64 and 4.68 times, respectively. Furthermore, cytotoxicity assays demonstrated that Exo-HK exerted nearly 4–5 times higher inhibitory effect against cancer cells than free HNK, thereby significantly enhancing its anticancer activity. Nonetheless, these studies have been confined to the cellular level, and further evaluation and improvement of Exo-HNK in animal models are imperative. Additionally, exploring strategies for HNK delivery using exosomes derived from other cell types represents a promising avenue for future research.

Transfersomes

Transfersomes represent a novel type of drug delivery system characterized by an aqueous core wrapped in a phospholipid bilayer and single-chain surfactants. The inclusion of single-chain surfactants improves the elasticity and deformability of transfersomes, also known as flexible liposomes.[64] In one study, Yasmeen et al prepared HNK-loaded transfersomes (HKTS) using an improved heating method based on green synthesis, resulting in a sustained release

effect.[54] HKTS exhibited remarkable elasticity, as evidenced by a deformation index of 13.9 ± 0.9 mL/s, notably higher than conventional liposomes (3.94 ± 1.2 mL/s). Moreover, HKTS were found to alleviate tumor immunosuppression by down-regulating transforming growth factor-β, making them a promising candidate for localized therapy of melanoma. However, the effect of HKTS on other cytokines in the tumor microenvironment remains to be studied, and further in vivo experiments are needed to investigate its efficacy.

Nanoparticles

Nanoparticles encompass inorganic or organic particles that typically range in size from 10 to 1000 nm. These particles possess the ability to improve drug metabolism, enhance drug specificity, and increase drug uptake by altering the biological distribution of pharmaceutical agents and facilitating targeted and controlled delivery.[65] In recent years, numerous nanoparticle-based carrier systems for HNK delivery have been reported, including polymeric nanoparticles, inorganic nanoparticles, and protein nanoparticles (Table 2).

Ji's team prepared carrier-free HNK self-assembled nanoparticles (SA) through hydrogen bonding and drug hydrophobic interactions, capitalizing on the amphiphilic structure of HNK (Figure 2A).[17] The $AUC_{(0-t)}$ of SA was notably higher at 3651.11 ng/mL·h, demonstrating a 2.29-fold increase than free HNK (1592.75 ng/mL·h). This points to the significant enhancement in bioavailability achieved by SA. Additionally, SA displayed noteworthy enhancements in antitumor immunity and exhibited significant selectivity towards the p53 pathway. In another study, Gou et al utilized Pluronic F127 as a surfactant to prepare HNK nanoparticles via the emulsion solvent evaporation method, notably improving the water dispersibility of HNK.[66] Additionally, Wu et al successfully prepared HNK nanoparticles to enhance the solubility and bioavailability of HNK, resulting in a significantly enhanced inhibitory effect on HepG2 cells.[67]

Polymeric Nanoparticles

Commonly utilized polymers for HNK delivery encompass PEG, PLA, poly (lactic-acid-glycolic acid) copolymer (PLGA), polycaprolactone (PCL), and pectin.

Qian et al prepared HNK-loaded PCEC nanoparticles using the solvent diffusion method, yielding a drug loading rate of approximately 20% alongside remarkable sustained release properties.[68] They also employed a solvent extraction approach to fabricate MPEG-PLA nanoparticles for HNK delivery, effectively enhancing the water solubility of HNK.[69] Another study synthesized HNK carbon dots by the hydrothermal synthesis method, demonstrating stable antibacterial properties and excellent biocompatibility.[70] Tang et al developed HNK-loaded chitin polymeric nanoparticles functionalized with EGCG (CE-HK) through ionic crosslinking.[71] At a dose of 40 mg/kg, CE-HK exhibited a tumor inhibition rate of 83.55%, significantly surpassing free HNK (30.15%), indicating a substantial improvement in antitumor efficacy. He and coworkers activated γ-CD metal-organic framework (CD-MOF) by supercritical carbon dioxide technology, increasing the surface area and pore volume to facilitate HNK delivery.[72] The drug loading rate of HNK@CD-MOF was as high as 40.78 ± 2.07 wt%, and its apparent solubility was 19.9-fold higher than free HNK. Moreover, HNK@CD-MOF promoted cellular uptake and transport of HNK in intestinal epithelial cells, significantly augmenting oral bioavailability.

In another study, chitosan/SCD nanoparticles were developed for ocular delivery of HNK.[73] The resulting HKCS-NPs displayed excellent ocular tolerance with no obvious ocular inflammation or pathological changes observed in rabbit eyes. Furthermore, the area under the concentration-time curve of HKCS-NPs was 1.59 times higher than free HNK, demonstrating enhanced ocular bioavailability. Weng et al formulated HNK-loaded nanoparticles using a novel biodegradable polysaccharide, HZ0223AP-PPT, as the carrier material.[74] These nanoparticles demonstrated excellent stability and safety, facilitating drug-controlled release in vitro.

Researchers have also investigated the utilization of polymer nanoparticles for targeted and co-delivery of HNK. Zhang et al developed self-assembled pectin nanoparticles containing galactose residues for HNK delivery, resulting in targeted delivery to asialoglycoprotein receptor-positive HepG2 cells and displaying higher cytotoxicity compared to free HNK.[76] Similarly, Yang et al prepared HNK-loaded nanoparticles (ATNH) utilizing PCEC as a carrier and incorporating FA modification through polyethyleneimine to target HNE-1 nasopharyngeal cancer cells, expressing high levels of FA receptors.[77] These nanoparticles successfully targeted tumor cells, significantly enhancing the anti-nasopharyngeal carcinoma effect. Furthermore, protein-polysaccharide hybrid nanoparticles were designed to co-deliver HNK, PMT,

Table 2 Summary of HNK-Loaded Nanoparticles

Classification	Materials/Co-Delivery/ Targeting Moiety	Preparation Methods	Physicochemical Properties	Cells	Animal Models	Main Results	Ref.
Nanoparticles	NA	Self-assembly	PS: ~98 nm; ZP: −41.7 mV	HT-29; SW480; MCF-7; MDA-MB-231; H1299; SKOV3; Caco-2; Hela; RAW264.7; HCT116 p53 (−/−); HCT116 p53 (+/+)	HT-29 xenograft tumor-bearing mice	Sustained drug release; efficient immunotherapy; synergistic anticancer effect	[17]
	Pluronic F127	Emulsion solvent evaporation method	PS: 33 nm; ZP: −0.385 mV	NA	NA	Improved water dispersibility	[66]
	Hydroxypropyl methylcellulose	Liquid antisolvent precipitation method	PS: 100–120 nm	HepG2	NA	Improved solubility and oral bioavailability; enhanced cytotoxicity	[67]
Polymeric nanoparticles	PCEC copolymer	Solvent diffusion method	PS: 80 nm; ZP: −3.8 mV; EE: 99%; DL: 20%	HEK293; A2780s; A2780cp	NA	Sustained drug release; inhibited cell proliferation	[68]
	MPEG-PLA copolymer	Solvent extract method	PS: 80 nm; ZP: ~−11.3 mV; DL: 10%	A2780s	NA	Enhanced solubility; inhibited cell proliferation	[69]
	Anhydrous ethanol	Hydrothermal synthesis method	PS: 11 nm	NA	NA	Stable antibacterial ability; excellent biocompatibility	[70]
	EGCG, chitin	Ionic crosslinking method	PS: 80 nm; ZP: 33.8 mV; DL: 22%	LO2, MRC-5, HK-2; A549; HepG2	HepG2 xenograft tumor-bearing mice	Increased cytotoxicity; enhanced anticancer effect	[71]
	Potassium hydroxide, γ-CD, PEG_{20000}	$ScCO_2$-assisted impregnation method	DL: ~40.78 wt%	Caco-2	NA	Improved solubility and bioavailability; enhanced cellular uptake and drug transport	[72]
	HK-SCD complex, chitosan	Ionic gelation method	PS: 373–523 nm; ZP: 19.9–24.2 mV; EE: 84.92%	NA	NA	Improved ophthalmic bioavailability; sustained drug release	[73]
	HZ0223AP-PPT	Hydrophilic polymer coagulation method	PS: ~198.50 nm; ZP: ~−52.60 mV; EE: ~77.75%; DL: ~13.46%	NA	NA	Improved solubility; stable release	[74]
	PEG_{45}, first generation OEG dendrons, second generation OEG dendrons	Evaporation-ultrasonication method	PS: 109.2–318.1 nm; ZP: −29.9 to −42.9 mV; DL: 39.6–73.7%	4T1	4T1 tumor-bearing mice	Smaller diameters exhibited higher antitumor efficacy	[75]
	HP-β-CD, pectin (targeting moiety: pectin)	Solution stirring method	PS: ~640.50 nm; ZP: ~−14.9 mV; EE: ~52.89%; DL: ~39.71%	HepG2; A549	NA	Sustained drug release; ASGR-positive HepG2 cells targeting; higher cytotoxicity	[76]

(*Continued*)

https://doi.org/10.2147/IJN.S431409

Table 2 (Continued).

Classification	Materials/Co-Delivery/ Targeting Moiety	Preparation Methods	Physicochemical Properties	Cells	Animal Models	Main Results	Ref.
	PCEC-PEI-FA copolymer (targeting moiety: FA)	Emulsion solvent evaporation method	PS: ~188.34 nm; EE: ~78.25%; DL: ~6.26%	HNE-1	HNE-1 xenograft tumor bearing mice	Sustained drug release; tumor targeting; enhanced anticancer activity	[77]
	Lf-RST conjugate, PMT-ALG conjugate, genipin (co-delivery: RST, PMT)	Solvent evaporation and crosslinking methods	PS: ~258.7 nm; ZP: ~−45.3 mV; EE: 93.3%; DL: 6.11%	MCF7; EAT	EAT tumor-bearing mice	Increased cellular uptake and cytotoxicity; synergistic antitumor effect	[78]
	PALA-g-mPEG, HNK-DMXAA conjugate (co-delivery: DMXAA)	Steglich esterification	PS: ~117.2 nm; ZP: ~−12.8 mV	HUVEC; 4T1	4T1 tumor-bearing mice	GSH-responsive drug release; enhanced antitumor activity	[33]
	PBAE, SPC, DSPE-PEG_{2000}, FA-DSPE-PEG_{2000} (targeting moiety: FA)	Emulsion solvent evolution method	PS: ~116.4 nm; ZP: ~−8.9 mV; EE: ~75.2%; DL: ~10.9%	4T1	4T1 tumor-bearing mice	pH-sensitive drug release; tumor targeting; enhanced antitumor and anti-metastasis effect	[79]
Inorganic nanoparticles	Mesoporous silica	Solvent-based method	NA	VSMC	Common carotid artery balloon injury rats	Higher suppression of intimal thickening	[80]
	mTiO_2, polypyrrole	Solution stirring method	DL: ~6.5%	HepG2; 4T1	4T1 tumor-bearing mice	Ultrasound/photoacoustic imaging; synergistic antitumor effect	[28]
	HK-CPT, GO, chitosan (co-delivery: CPT; targeting moiety: FA)	Solution stirring method	NA	MCF-7	NA	Enhanced solubility; increased cytotoxicity	[81]
Protein nanoparticles	Zein, Tween 80 (targeting moiety: HA)	Antisolvent precipitation and electrostatic deposition methods	PS: 210.4 nm; ZP: ~−34.54 mV; EE: 88.1–93.6%	4T1	4T1 tumor-bearing mice	Tumor targeting; improved anticancer and anti-metastasis effect	[82]
	Zein, Tween 80 (targeting moiety: PSA)	Antisolvent precipitation and electrostatic deposition methods	PS: ~107.2 nm; ZP: ~−33.5 mV; EE: ~79.2%; DL: ~7.3%	4T1	4T1 tumor-bearing mice	Tumor targeting; improved anticancer and anti-metastasis effect	[83]
	PVP, BSA, dopamine (targeting moiety: FA)	Solvent evaporation method	PS: ~184.82 nm; ZP: ~11.82 mV	4T1	4T1 tumor-bearing mice	pH-sensitivity drug release; tumor targeting; enhanced antitumor activity	[84]
	HNK prodrug, TPGS, BSA	Nanoprecipitation method	PS: ~144.60 nm; ZP: ~−22.63 mV; EE: ~88.65%; DL: ~59.12%	LLC; MCF-7	LLC xenograft tumor-bearing mice	Prolonged blood circulation; improved antitumor efficiency	[85]

Abbreviations: PCEC, poly(ε-caprolactone)-poly(ethylene glycol)-poly(ε-caprolactone); PLA, poly(lactic acid); SCD, sulfobutylether-β-cyclodextrin; PEI, polyethylenimine; FA, folate; EGCG, epigallocatechin-3-gallate; PALA-g-mPEG, PEGylated poly(alpha-lipoic acid) copolymer; DMXAA, 5.6-dimethylxanthenone-4-acetic acid; GSH, glutathione; γ-CD, γ-cyclodextrin; PBAE, poly (β-amino) ester; OEG, oligo(ethylene glycol); RST, rosuvastatin; PMT, pemetrexed; ALG, alginate; CPT, camptothecin; GO, graphene oxide; PVP, polyvinylpyrrolidone; BSA, bovine serum albumin; TPGS, tocopherol polyethylene glycol succinate.

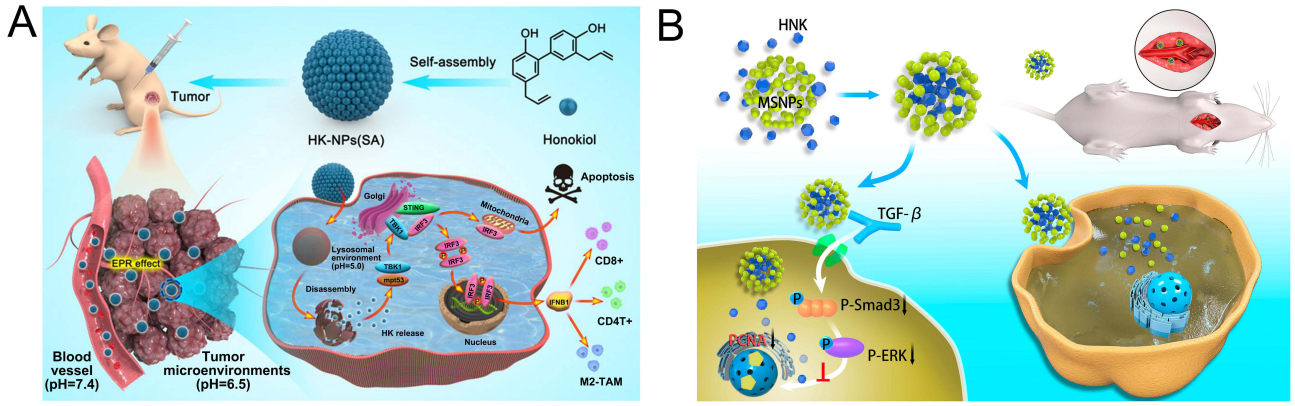

Figure 2 (**A**) Schematic diagram illustrating the mechanism of carrier-free HNK self-assembled nanoparticles. Reprinted from Ji H, Wang W, Li X, et al. Natural small molecules enabled efficient immunotherapy through supramolecular self-assembly in p53-mutated colorectal cancer. *Acs Appl Mater Interfaces*. 2022;14(2):2464–2477. Copyright (2022). American Chemical Society.[17] (**B**) Schematic diagram illustrating the mechanism of HNK-MSNPs. Reprinted from Wei X, Fang Z, Sheng J, Wang Y, Lu P. Honokiol-mesoporous silica nanoparticles inhibit vascular restenosis via the suppression of TGF-β signaling pathway. *Int J Nanomedicine*. 2020;15:5239–5252. Creative Commons.[80]

and RST.[78] Compared with free HNK, these hybrid nanoparticles exhibited significantly increased uptake in MCF-7 cells, resulting in an 8-fold decrease in IC_{50} and exhibiting the most potent anticancer effect.

The responsive release of HNK from polymer nanoparticles can be achieved by utilizing specific materials. In a study, HNK was conjugated with DMXAA, a STING agonist, and then grafted onto GSH-responsive poly (α-lipoic acid)-polyethylene glycol copolymers, resulting in the development of GSH-responsive nanoparticles (H-D NPs).[33] H-D NPs demonstrated the ability to selectively release HNK and DMXAA in response to elevated levels of GSH present in tumor cells, achieving a combined therapy of tumor cells inhibition by HNK and tumor blood supply blockage by DMXAA. Furthermore, H-D NPs exhibited an impressive suppression rate of 93% against 4T1 tumor-bearing mice, remarkably surpassing the efficacy of the combination of HNK and DMXAA (82.6%), HNK alone (13.4%) and DMXAA alone (76.6%). Another approach involved the design of lipid-polymer hybrid nanoparticles (termed FA/PBAE/Hol-NPs) with a pH-sensitive PBAE as the core, encapsulating hydrophobic HNK and further modifying it with FA.[79] The release rates of FA/PBAE/Hol-NPs over 8 hours at pH 7.4 and 5.5 were determined to be 42.7% and 92.6%, respectively, demonstrating pH-responsive release behavior. Due to the specific interaction of FA with the abundantly expressed FA receptors on the surface of 4T1 cells, Coumarine-6-labeled FA/PBAE-NPs demonstrated the highest uptake throughout the observation period. In addition, FA/PBAE/Hol-NPs exhibited the capacity to inhibit migration and invasion. Remarkably, in a 4T1 breast cancer mouse model, these nanoparticles displayed significant inhibitory effects on both primary breast cancer and lung metastasis, resulting in tumor inhibition rates of 62.8% and 84.3%, respectively. Nevertheless, it is essential to take into account the influence of polymer molecular weight and stability on the ultimate delivery efficacy, as well as the potential toxicity associated with surfactants during the preparation process.

Inorganic Nanoparticles

Inorganic nanoparticles are typically derived from diverse materials, including metals, oxides, semiconductors, and carbon-based structures. These nanoparticles offer distinct advantages owing to their exceptional physical stability, extensive surface area, superior catalytic performance, and responsiveness to optical, magnetic, and ultrasonic signals.[86]

Wei et al fabricated HNK-loaded mesoporous silica nanoparticles (HNK-MSNPs) to inhibit vascular restenosis (Figure 2B).[80] HNK-MSNPs effectively suppressed the proliferation and migration of vascular smooth muscle cells by attenuating the phosphorylation of Smad3. In a rat balloon injury model, HNK-MSNPs exhibited superior inhibition of intimal hyperplasia compared to free HNK. In a separate study, He et al designed HNK-loaded mesoporous TiO_2 nanocomposites coated with polypyrrole ($mTiO_2$@PPY) for a multifunctional approach involving chemotherapy, sono-dynamic therapy, photothermal therapy, and dual-modality ultrasound/photoacoustic imaging of tumors.[28] Notably, it displayed ultrasonic and photoacoustic imaging properties both in vivo and in vitro, with the ultrasonic signal intensity increasing in correlation with the concentration of $mTiO_2$@PPY. In a 4T1 breast cancer model, following 5 minutes of

laser irradiation, the $mTiO_2$@PPY-HNK group experienced a substantial temperature increase within the tumor region, elevating from 35°C to 46°C. Conversely, the control group exhibited no noticeable temperature rise. Furthermore, after a 16-day treatment period, the $mTiO_2$@PPY-HNK + laser + US group achieved substantial tumor ablation in comparison to other groups, confirming the potent antitumor effects of this multifunctional drug delivery system combining photothermal, sonodynamic, and chemotherapy approaches. In another investigation, a combinatorial drug of HNK and CPT was loaded onto chitosan-functionalized GO nanoparticles and modified with FA, which greatly enhanced the inhibitory effects on MCF-7 breast cancer cells.[81] Inorganic nanoparticles have great potential in HNK delivery, but their structural characteristics and morphology significantly impact drug loading rates, release kinetics, and therapeutic properties. Consequently, further research is imperative to gain better control over these structural parameters. Moreover, there is a noticeable gap in the literature regarding the utilization of metal nanoparticles for HNK delivery, which may be attributed to concerns about the potential toxicity of metal nanoparticles caused by the use of organic solvents in the synthesis process. However, in recent years, numerous studies have focused on synthesizing metal nanoparticles using natural reducing, capping, and stabilizing agents.[87–91] These advancements offer a promising avenue for researchers, and we anticipate a growing trend in utilizing metal nanoparticles for HNK delivery.

Protein Nanoparticles

Zein, a natural amphiphilic plant protein, was utilized to fabricate HNK-loaded zein nanoparticles by the antisolvent precipitation method and functionalized them with HA and PSA,[82,83] respectively. The resulting HA-Zein-HNK and PSA-Zein-HNK exhibited enhanced anti-proliferative and pro-apoptotic capabilities against 4T1 cells, effectively suppressing their migration and invasion. In vivo studies demonstrated that both types of nanoparticles exerted targeted distribution in tumor tissues, leading to remarkable antitumor effects and significant inhibition of lung and liver metastasis.

BSA is a widely utilized animal protein in drug delivery systems. Yu et al prepared polydopamine-coated nanoparticles loaded with HNK using BSA and PVP, which were further modified with FA to obtain HK-PDA-FA-NPs.[84] In a 4T1 breast cancer model, the HK-PDA-FA-NPs exhibited a remarkable tumor inhibition rate of 79.34%, surpassing that of the HK-NPs group (69.54%). In another approach, the researchers designed a prodrug nanoparticle system (HP-NPs) capable of forming a complex with albumin in vivo.[85] The study revealed that the HNK prodrug (HP) rapidly formed a covalent conjugate with the sulfhydryl group of albumen, enabling a sustained release of HNK in LLC cells. Compared with free HNK, HP-NPs considerably augmented the area under the concentration-time curve (26.5 times higher), mean retention time (7.2 times higher), and tumor accumulation (9.74 times higher). Additionally, LLC xenografted lung cancer mice treated with HP-NPs displayed the smallest tumor volume and tumor burden rate, indicating the potent anticancer efficacy of HP-NPs in enhancing the therapeutic effects of HNK.

Polymeric Micelles

Polymeric micelles, characterized by a core-shell structure formed through the self-assembly of amphiphilic block copolymers, offer exceptional biocompatibility and possess the ability to enhance drug solubility while prolonging drug half-life.[92] Commonly utilized polymers in the preparation of HNK micelles encompass MPEG-PCL, mPEG-PLA, poly(2-ethyl-2-oxazoline)-poly ($_{D,\ L}$-lactic acid) (PEOz-PLA), Pluronic F-127, PCEC (Table 3).

Block Micelles Based on MPEG-PCL

Gou et al prepared self-assembled micelles of MPEG-PCL block copolymers to encapsulate HNK using an ultrasonic-assisted direct dissolution method.[93] The resulting micelles displayed a diameter of 31.16 ± 0.93 nm and a drug loading capacity of 20%. In vitro studies demonstrated sustained release behavior and improved solubility of HNK. HNK-loaded MPEG-PCL micelles were applied in another study to address age-related macular degeneration.[94] The micelles exhibited periodic down-regulation of vascular endothelial growth factor and anti-hypoxia-inducible factor expression. Cheng's team prepared HNK-loaded biodegradable micelles, demonstrating superior efficacy in inhibiting tumor cell proliferation, promoting cell apoptosis, and suppressing angiogenesis compared to free HNK.[95]

Combination chemotherapy has always been recognized as a promising strategy for combating tumors. Researchers successfully co-encapsulated HNK and DOX within MPEG-PCL micelles, forming DOX-HK-M.[96] The findings revealed

Table 3 Summary of HNK-Loaded Polymeric Micelles

Copolymer	Combined Therapy/Targeting Moiety	Preparation Methods	Physicochemical Properties	Cells	Animal Models	Main Results	Ref.
MPEG-PCL	None	Direct dissolution method assisted by ultrasound	PS: ~31.16 nm; EE: ~65.40%; DL: ~20.74%	A2780s; HEK293; L929	NA	Sustained drug release	[93]
	None	Solvent evaporation method	PS: ~30.8 nm; ZP: ~−5.46 mV; EE: ~64%	ARPE-19	NA	Sustained drug release; downregulation of HIF and VEGF	[94]
	None	Self-assembly method	PS: ~35.7 nm; ZP: ~−3.3 mV; EE: ~96.1%; DL: ~19.22%	UMR106	UMR106 tumor-bearing mice	Sustained drug release; enhanced antitumor efficiency	[95]
	Co-delivery: DOX	Self-assembly method	PS: 34 nm; ZP: −2.3mV; EE: 99.8%; DL: 5%;	U87; C6	C6 tumor-bearing mice; U87 xenograft tumor-bearing zebrafish	Sustained drug release; synergistic antitumor effect	[96]
	Co-delivery: PTX	Solid dispersion method	PS: ~28.7 nm; ZP: ~−1.42 mV; EE: ~98.2%; DL: ~9.4%	4T1; HEK 293	4T1 tumor-bearing mice	Sustained drug release; increased tumor accumulation; synergistic antitumor effect	[29]
mPEG-PLA	Co-delivery: sirolimus	Thin-film dispersion method	PS: ~60.4 nm; EE: ~84.3%; DL: ~8.5%	Caco-2	NA	Improved oral transport of sirolimus; inhibited P-gp	[97]
	Co-treatment: CXB	Thin film dispersion method	PS: ~33.81 nm; ZP: ~−13.50 mV; EE: ~96.47%; DL: ~8.77%	4T1	4T1 tumor-bearing mice	Sustained drug release; improved antitumor effect	[98]
PEOz-PLA	Co-delivery: PTX	Film-hydration method	PS: ~44.12 nm; EE: ~79.6%; DL: ~3.6%	MCF-7/ADR; MDA-MB-231; MDA-MB-231-luc-GFP	MDA-MB-231-luc-GFP xenograft tumor-bearing mice	pH-sensitive drug release; inhibited multidrug resistance and metastasis	[99]
	Co-delivery: DOX	Film hydration method	PS: ~20.86 nm; EE: ~57.90%; DL: ~6.64%	MDA-MB-231; MDA-MB-231-luc-GFP	MDA-MB-231-luc-GFP xenograft tumor-bearing mice	pH-sensitive drug release; inhibited tumor growth and metastasis	[100]
Pluronic F-127	None	Emulsion-solvent evaporation method	PS: ~37.92 nm; ZP: ~1.98 mV; EE: ~92.30%; DL: ~8.45%	NA	NA	Improved pharmacokinetic parameters; sustained drug release; increased solubility	[101]
	NA	Emulsion-solvent evaporation method	PS: ~38.89 nm; ZP: ~13.43 mV; EE: ~87.54%; DL: ~12.51%;	16HBE; L-02	NA	Sustained release; increased solubility; improved pharmacokinetic parameters	[102]
	Targeting moiety: biotin	Dialysis method	PS: ~210.9 nm; ZP: ~12.9 mV; EE: ~70.79%; DL: ~9.70%	B16	NA	Sustained drug release; targeted delivery; higher cytotoxicity	[103]
PECE	None	Direct dissolution method assisted by ultrasound	PS: 58 nm; ZP: −0.4 mV; DL: 6.7%	A549; HEK293; CT26	NA	Sustained drug release; increased solubility	[104]
PCEC	None	Direct dissolution method assisted by ultrasonication	PS: 61 nm; ZP: −0.502 mV; EE: 50%; DL: 4.8%	A549	NA	Sustained drug release	[105]

(*Continued*)

https://doi.org/10.2147/IJN.S431409

Table 3 (Continued).

Copolymer	Combined Therapy/Targeting Moiety	Preparation Methods	Physicochemical Properties	Cells	Animal Models	Main Results	Ref.
PCL-b-PEG	None	Direct dissolution method assisted by ultrasound	PS: 40 nm; ZP: 8.36 mV; EE: 16.01%; DL: 7.41%	A549; CT26	NA	Sustained drug release; increased water solubility	[106]
MPEG	None	Thin-film hydration, followed by extrusion method	PS: 9.21 nm; ZP: −6.20 mV	LL/2	NA	Enhanced solubility	[107]
TPGS	None	Thin-film hydration method	PS: 36 nm; ZP: −34.31 mV; EE: 91.5%	MDA-MB-231, MDA-MB-453; MDA-MB-468; Caco-2	Orthotopic MDA-MB-231 xenograft tumor-bearing mice	Increased oral bioavailability; enhanced antitumor effect	[108]
Rebaudioside A	None	Thin-film hydration method	PS: ~4.356 nm; ZP: ~−3.39 mV; EE: 65.7−97.8%	HuH-7H22; H22	H22 tumor-bearing mice	Improved oral bioavailability; enhanced antitumor effect	[109]
Dextran	Co-delivery: PTX	Dialysis method	PS: 100–120 nm; ZP: −15 to −20 mV; DL: ~1.01%	Hep-2	Hep-2 xenograft tumor-bearing mice	GSH/ROS dual responsive drug release; synergistic antitumor effect	[110]
Lecithin, sodium, deoxycholate	Co-delivery: magnolol	Thin film dispersion method	PS: ~118.4 nm; ZP: ~−63.7 mV; EE: 96.41%; DL: 44.42%	NA	NA	Improved solubility and oral bioavailability	[111]
Soluplus, $TPGS_{1000}$, DSPE-PEG_{2000}-DQA	Co-delivery: PTX; targeting moiety: DQA	Film dispersion method	PS: ~91.22 nm; EE: ~89.75%	LLT	LLT tumor-bearing mice	Suppressed VM channels and tumor metastasis; synergistic antitumor effect	[112]
HA-deoxycholic acid copolymer	Co-delivery: Gem-C_{12}; targeting moiety: HA	Thin film dispersion method	PS: 53.36 nm; ZP: −37.6 mV; EE: ~86.3%; DL: 2.8%	U87; B16F10; HK2	U87 xenograft tumor-bearing mice	Tumor targeting; enhanced antitumor effect	[113]

Abbreviations: PTX, paclitaxel; HIF, hypoxia inducible factor; CXB, celecoxib; PECE, poly(ethylene glycol)–poly(ε-caprolactone)–poly(ethylene glycol); DQA, dequalinium; Gem-C_{12}, lauroyl-gemcitabine; ROS, reactive oxygen species.

that the inclusion of HNK effectively augmented the anti-glioma activity of DOX. Notably, both tumor xenograft zebrafish and glioma mice treated with DOX-HK-M exhibited the smallest tumor volumes. In a separate investigation, Wang et al developed MPEG-PCL micelles co-loaded with PTX and HNK (P-H/M) by a solid dispersion method for synergistic breast cancer treatment.[29] The tumor volume of 4T1 tumor-bearing mice subjected to P-H/M treatment (557.64 ± 243.81 mm^3) was remarkably smaller compared to those treated with PTX/M (932.70 ± 256.43 mm^3) or HNK/M (1463.77 ± 148.74 mm^3), highlighting the augmented anti-breast cancer effects achieved by P-H/M.

Block Micelles Based on mPEG-PLA

Sirolimus is a recognized substrate of P-gp, and previous studies have demonstrated the inhibitory effect of HNK on P-gp.[114] Li et al prepared mPEG-PLA micelles co-loaded with sirolimus and HNK.[97] The inclusion of HNK significantly increased the apparent transport coefficient of sirolimus from apical to basolateral in Caco-2 cells. Furthermore, the researchers utilized mPEG-PLA/vitamin E-TPGS composite micelles to encapsulate CXB (PV-CXB) and HNK (PV-HNK), enabling a combined treatment against breast cancer.[98] The PV-CXB and PV-HNK combination therapy exhibited notable outcomes, including the smallest tumor volume, lowest tumor weight, highest tumor cell apoptosis rate, and significantly reduced the expression of various tumor growth markers.

Block Micelles Based on PEOz-PLA

Liu's team prepared pH-sensitive PEOz-PLA micelles to co-deliver PTX and HNK.[99] As a result, HNK exhibited effective down-regulation of P-gp expression in the multidrug-resistant human breast cancer cell line MCF-7/ADR, resulting in enhanced cytotoxicity and a remarkable reversal effect on multidrug resistance. Although these micelles effectively inhibited tumor cell invasion and metastasis, the synergistic effect of HNK and PTX was not yet optimal. Consequently, an acid-sensitive benzoic imine linker was employed to conjugate PEOz-PLA with DOX, and HNK was subsequently encapsulated within the hydrophobic core, leading to the formation of double-drug-loaded micelles (HNK/PP-DOX-PM).[100] The release rates of DOX within the first 30 min were about 21% and 47% at pH 7.4 and 5.0, respectively. Notably, HNK/PP-DOX-PM exhibited enhanced antitumor and anti-breast cancer metastasis effects while reducing the toxic side effects of DOX.

Block Micelles Based on Pluronic 127

Feng's group conducted several studies to improve the solubility and targeted delivery of HNK using Pluronic127 micelles.[101–103] Two strategies were employed to encapsulate HNK within the micelles: Pluronic127-cyclodextrin conjugate (F127-CD) and chitosan-Pluronic127 conjugate (F127-CS).[101,102] Both HNK-loaded micelles exhibited sustained-release behavior, and the encapsulation with F127-CD demonstrated a remarkable increase in the water solubility of HNK to 1.013 mg/mL, which was over 18 times than free HNK. Similarly, encapsulation with F127-CS significantly increased the water solubility of HNK to 1.46 mg/mL, which was over 27 times compared to free HNK. Moreover, a targeted delivery system for HNK was developed by utilizing biotin-modified F127-CS conjugate as carriers, resulting in the formulation of HNK-loaded micelles (Honokiol-F127-CS-BIO).[103] The study demonstrated a significantly stronger fluorescence signal in the FITC-F127-CS-BIO group compared to the unmodified biotin group, with fluorescence intensity increasing over time. This observation indicated that biotin-biotin receptor-mediated endocytosis facilitated enhanced cellular uptake by B16 cells. The IC_{50} values of the free HNK, Honokiol-F127-CS, and Honokiol-F127-CS-BIO against B16 cells were 7.51, 9.46, and 3.03 μg/mL, respectively, indicating a significant enhancement of cytotoxicity achieved with Honokiol-F127-CS-BIO.

Block Micelles Based on Other Copolymers

Qian and colleagues prepared HNK-loaded PECE and PCEC block micelles using an ultrasound-assisted direct dissolution method, effectively increasing the solubility of HNK and exhibiting sustained release properties.[104,105] Additionally, the team developed biodegradable HNK-loaded PCL-b-PEG micelles,[106] which demonstrated excellent water dispersibility and sustained-release behavior, with a cumulative release rate of 32% at 72 hours, compared to approximately 74%

of the free HNK group. In another study, MPEG-HNK conjugates were synthesized to form nano-micelles with an average particle size of less than 20 nm, significantly improving HNK solubility.[107]

A TPGS-based nano-micelle system for encapsulating HNK (HNK-NM) has been investigated in previous studies.[108] In oral administration at doses of 40 and 80 mg/kg, compared with free HNK, the HNK-NM group exhibited a 4.06- and 3.60-fold increase in C_{max}, a 6.26- and 5.83-fold increase in AUC, and a 1.78- and 2.08-fold decrease in tumor volume, respectively. These findings indicated a substantial improvement in the oral bioavailability and anti-triple negative breast cancer effect of HNK. Wang et al prepared self-assembled micelles based on Rebaudioside A (RA-HK), leading to a 396.22-fold increase in HNK solubility.[109] Pharmacokinetic analysis revealed that the C_{max} and AUC_{0-24} values of the RA-HK group were 2.14 and 1.66 times higher, respectively, compared to the HNK group. Moreover, the tumor inhibition rates in H22 solid tumor mice treated with RA-HK at doses of 50 and 100 mg/kg were 43.11% and 72.77%, respectively, surpassing the 30.72% observed in the 100 mg/kg free HNK group.

Zhou et al developed a novel strategy for laryngeal cancer treatment by conjugating dextran with PTX and HNK through a selenium bond, resulting in the self-assembly of a polymer prodrug micelle (PHPPM).[110] PHPPM exhibited dual responsiveness to ROS and GSH. After 12 hours of administration, the blood concentration was about 6.5 μg/mL, whereas the free drug group was quickly cleared within 4 hours. Notably, the PTX and HNK concentrations in tumor tissue of the PHPPM group were 3.82- and 4.31-fold higher, respectively, compared to the free drug group. This substantial increase in drug accumulation and prolonged circulation time indicated enhanced tumor targeting. In an in vivo pharmacodynamic study, the tumor inhibition rate of the PHPPM group reached 81.3%, markedly surpassing that of the free drug group and demonstrating the synergistic antitumor effect. In a separate study, Lin et al prepared mixed polymer micelles co-loaded with HNK and magnolol based on lecithin, effectively improving the solubility and oral bioavailability of the drug.[111]

Improving the targeting ability of drugs is crucial in optimizing therapeutic efficacy. Researchers have employed Soluplus and $TPGS_{1000}$ to develop polymer micelles co-loaded with PTX and HNK, which were further modified with DQA for lung cancer treatment.[112] These polymer micelles effectively suppressed angiogenic mimicry channels and tumor metastasis while selectively accumulating at tumor sites, resulting in a remarkable antitumor effect. In a related study, Liu et al developed copolymer micelles based on HA-deoxycholic acid and co-loaded with lauryl gemcitabine and HNK (HA-M) for the combined chemotherapy of gliomas.[113] The results suggested that DiD-labeled HA-M exhibited the highest accumulation in tumor tissues through CD44-mediated endocytosis. Besides, the tumor inhibitory effect of the HA-M group was the most potent, leading to a significant extension of the median survival time in mice by 50 days compared to the free drug group.

Nanogels

Nanogels are nanoscale three-dimensional hydrogels formed by cross-linking of swelling polymers with excellent water retention capacity. These versatile structures can be engineered to possess responsive properties, such as temperature-responsive, light-responsive, or pH-responsive, depending on the specific environmental stimuli (Table 4).[115]

Nanogels

Green self-assembled nanogels, constructed from natural polysaccharides and proteins, are promising delivery systems. The PMT-Lf conjugate was assembled into CMC to form nanogels, which were further utilized to encapsulate the inclusion complex of HNK and β-cyclodextrin, leading to the development of a dual-drug delivery system termed P/H-Lf-CMC NGs.[30] In MDA-MB-231 breast cancer cells, the RBITC-labeled Lf-CMC NGs exhibited more potent red fluorescence than free RBITC in a time-dependent manner, indicating that the modification of Lf enhanced cellular uptake. Moreover, the tumor volume of the P/H-Lf-CMC NGs group was 4 times smaller than the PMT plus HNK group, demonstrating an enhanced antitumor effect.

Table 4 Summary of HNK-Loaded Nanogels

Type	Materials/Combined Therapy/ Targeting Moiety	Preparation Method	Physicochemical Properties	Cells	Animal Models	Main Results	Ref.
Nanogels	PMT-Lf conjugate, CMC, HK-HPβCD (co-delivery: PMT; targeting moiety: Lf)	Chemical crosslinking and physical loading methods	PS: ~193.4 nm; ZP: ~−34.5 mV; EE: ~67.33%; DL: ~4.55%;	MDA-MB-231; A549; EAT	EAT tumor-bearing mice	Sustained drug release; tumor targeting; synergistic antitumor effect	[30]
Thermo-responsive hydrogel	PECE copolymer, Pluronic F127	Emulsion solvent evaporation and physical loading methods	HK-NP: PS: ~33.34 nm	LLC	LLC tumor-bearing cells	Suppressed MPE; enhanced antitumor effect; prolonged survival time	[116]
	PECE copolymer, Pluronic® F127	Emulsion solvent evaporation and physical loading methods	HK-NPs: PS: ~33.36 nm; ZP: ~−0.270 mV; EE: ~99.13%; DL: ~14.92%	SKOV3	SKOV3 xenograft tumor-bearing mice	Sustained drug release; enhanced antitumor effect; prolonged survival time	[117]
	Kolliphor®P407, PLGA-PEG-PLGA (co-treatment: PTX)	High-pressure homogenization and physical loading methods	HK-NS: PS: ~82.2 nm; DL: ~8.33 mg/mL	4T1	4T1 tumor-bearing mice	Sustained drug release; synergistic antitumor effect	[118]
pH/thermo-responsive hydrogel	PNIPAM-co-AA copolymer (targeting moiety: Lf)	Solvent evaporation method	PS: ~116.5 nm; ZP: ~−31.1 mV; EE: 77.7%; DL: 18.65 wt%	MCF-7; A549; EAT	EAT tumor-bearing mice	pH/thermo-sensitive drug release; tumor targeting; improved anticancer effect	[119]

Abbreviations: CMC, carboxymethyl cellulose; MPE, malignant pleural effusion; PNIPAM-co-AA, poly(*N*-isopropylacrylamide)-acrylic acid.

https://doi.org/10.2147/IJN.S431409

Thermo-Responsive Hydrogel

Qian's team has conducted extensive research on thermosensitive hydrogels containing HNK.[116,117,120–124] Their studies involved the development of PECE thermosensitive hydrogels loaded with HNK nanoparticles, aimed at improving the water solubility of HNK and enhancing its therapeutic effect against MPEs.[116] Following a 16-day treatment period, the HNK-hydrogel group exhibited a substantial reduction of 66.1% in pleural effusion volume, a significant decrease in tumor lesions, and a two-fold increase in survival time. Furthermore, the therapeutic potential of HK-NPs/hydrogel in ovarian peritoneal cancer was investigated.[117] The tumor inhibition rate of the HK-NPs/hydrogel group was 4 times higher than free HNK. Moreover, the median survival time of mice in the HK-NPs/hydrogel group reached 62 days, compared to 42 days for the free HNK group, thus significantly enhancing the anticancer effect.

To enhance drug accumulation at specific lesion sites, a localized drug delivery system was developed for the combined therapy of breast cancer.[118] The resulting HK-NS-Gel was designed as a controlled-release drug reservoir capable of gradually releasing HNK after intratumoral injection. Simultaneously, PTX was rapidly released to the tumor site through intravenous injection, thus facilitating synergistic anticancer effects. The combined treatment group demonstrated a 30% increase in tumor inhibition rate compared to the group receiving single treatment. Furthermore, the accumulation of PTX in the tumor was significantly enhanced, reaching levels 2–3 times higher than that observed in the single PTX injection group.

pH/Thermo-Responsive Hydrogel

To enhance the tumor-targeting capability of HNK, Metawea et al copolymerized pH-sensitive acrylic acid (AA) with thermosensitive poly(N-isopropylacrylamide) (PNIPAM) and further modification with Lf for HNK delivery.[119] The resulting HNK/Lf-PNIPAM-co-AA exhibited temperature-responsive release behavior of HNK at a constant pH, with a 19% higher release rate at 40°C than at 37°C. Similarly, it demonstrated pH-dependent release behavior of HNK at a constant temperature, with a release rate about 30% higher at pH 5.5 than at pH 7.4. HNK/Lf-PNIPAM-co-AA significantly enhanced the cytotoxicity against A549 and MCF-7 cells and facilitated targeted uptake by MCF-7 cells through Lf receptor-mediated endocytosis. In vivo experiments revealed that mice treated with HNK/Lf-PNIPAM-co-AA exhibited the smallest increase in tumor volume growth (138%) in comparison to the free HNK group (167%) and the positive control group (320%), significantly enhancing the tumor inhibitory effect of HNK.

Nanogels containing HNK have exhibited sustained and stimulus-response release properties. Nevertheless, achieving the desired therapeutic effect with a single stimulus-responsive nanogel presents a challenge, making the exploration of multiple stimuli for synergistic therapy a promising avenue for further research. Depending on the specific therapeutic applications, tailored responsive nanogels should be designed. For example, pressure-responsive nanogels could be developed for oral administration, while biomolecular- and light-responsive nanogels are suitable for in-situ tumor delivery.

Other NDDSs

Emulsions

Emulsions are composed of oil, water, surfactants, and co-surfactants. Incorporating hydrophobic drugs into the oil phase of these emulsions can enhance their solubility and bioavailability (Table 5).

In a study, an HNK and sirolimus co-delivered self-microemulsifying drug delivery system was prepared.[31] By inhibiting P-gp, HNK effectively reduced the efflux of sirolimus by approximately 35-fold, thereby substantially improving the oral absorption and transport. In another study, an HNK-loaded self-microemulsifying drug delivery system (Nano-HO) was developed for treating Alzheimer's disease.[125] Nano-HO exhibited a significant increase in the oral bioavailability of HNK and effectively alleviated the cognitive impairment of TgCRND8 mice compared to free HNK. In addition, Nano-HO demonstrated a more effective regulation of the gut microbiota. Gostyńska et al prepared an HNK-loaded nanoemulsion (H-NM) for intravenous administration in the treatment of glioblastoma.[126] The H-NM displayed excellent stability and enhanced cytotoxicity against T98G and UM-138 MG cells. The emulsion displayed the

Table 5 Summary of Other NDDSs for HNK

Type	Materials/Co-Delivery/ Targeting Moiety	Preparation Method	Physicochemical Properties	Cells	Animal Models	Main Results	Ref.
Emulsions	Cremophor EL, MCT, propylene glycol (co-delivery: sirolimus)	Spontaneous emulsification method	PS:18–23 nm	Caco-2	NA	Improved oral transport	[31]
	PEG-400, Kolliphor® HS-15, MCT	Solution stirring method	PS: ~23.30 nm; ZP: ~−6.19 mV	NA	TgCRND8 mice (Alzheimer's disease)	Improved oral bioavailability; modulated gut microbiota; improved cognitive impairments	[125]
	Lipofundin MCT/LCT 20%	Low-energy shaking method	MDD: ~201.4 nm; ZP: ~−28.5 mV	T98G; U-138 MG	NA	Good stability; enhanced cytotoxicity	[126]
Nanocapsules	Lf-QDs conjugate, CS-based nanocapsules (co-delivery: CXB; targeting moiety: CS, Lf)	Layer-by-layer assembly technique	PS: ~201.7 nm; ZP: ~6.16 mV; EE: 96.0%	MCF-7; MDA-MB-231; EAT	EAT tumor-bearing mice	Enhanced cytotoxicity and antitumor efficiency; provided imaging capability; tumor targeting	[127]
	PEG-PLGA, SPC, oil, Tween 80	Nanoprecipitation method	$PS_{(min)}$: 125 nm; $EE_{(max)}$: 94%	MCF-7; EAC	EAC xenograft tumor-bearing mice	Enhanced cytotoxicity; improved antitumor effect	[128]
Dendrimers	Codendrimer PGC	Evaporation method augmented by ultrasonication	PS: ~128.6 nm; ZP: ~63.9 mV; DL: 60 wt%	4T1	4T1 tumor-bearing mice	Sustained drug release; enhanced cytotoxicity; improved antitumor efficacy	[129]
	PAMAM	Codissolution method	DL: ~30.72%	HOKs	Caries rats	Sustained drug release; exhibited long-term anticaries and antibacterial effect	[32]
	$(TPG_3–OH)$-HK-LA-PEG conjugate, $(TPG_3–NH_2)$-SuHK-FA-SuPEG conjugate (targeting moiety: LA, FA)	Synthetic method	$(TPG_3–OH)$-HK-LA-PEG: PS: ~250.9 nm; ZP: ~−11.5 mV; DL: ~20.99% $(TPG_3–NH_2)$-SuHK-FA-SuPEG: PS: ~251.8 nm; ZP: ~−22.3 mV; DL: ~19.51%	Wi-38; Huh-7; HepG2	NA	Tumor cell targeting; enhanced cytotoxicity	[130]
Nanosuspensions	BSA, PVP	Solvent precipitation-ultrasonication method	PS: ~116.2 nm; ZP: ~−44.7 mV; DL: ~50.4%	H22	H22 tumor-bearing mice	Enhanced oral bioavailability; improved distribution in the cardio-cerebrovascular system	[131]
	Poloxamer 407	High pressure homogenization method	PS: ~30.1 nm; ZP: ~−12.16 mV; DL: ~96.9%	NA	Xylene-induced ear edema mice	Increased dissolution rate; enhanced anti-inflammatory ability	[132]
Nanofibers	PLGA, TFE	Electrospinning technology	PS: ~400 nm	786-O; ACHN	NA	Inhibited proliferation and migration	[133]
Nanodroplets	DSPE-PEG2000-GA, DPPC, Cholesterol, DSPE-PEG2000, PFP (targeting moiety: GA)	Thin film ultrasonic dispersion method	PS: ~324.8 nm; ZP: ~−29.9 mV; EE: ~83.15%; DL: ~7.92%	HepG2	HepG2 xenograft tumor-bearing mice	Enhanced cytotoxicity and cellular uptake; targeted antitumor activity and ultrasound imaging	[134]

Abbreviations: MCT, medium-chain triglycerides; Kolliphor® HS-15, PEG-15-hydroxystearate; LCT, long-chain triglycerides; MDD, mean droplet diameter; QDs, quantum dots; CS, chondroitin sulfate; LA, lactobionic acid; PAMAM, poly (amido amine); TFE, 2,2,2-trifluoroethanol; GA, glycyrrhetinic acid; DPPC, 1,2-dipalmitoyl-*sn-glycero*-3-phosphocholine; PFP, perfluoro-*n*-pentane.

https://doi.org/10.2147/IJN.S431409 DovePress

potential to improve the oral bioavailability of HNK significantly, while further investigations are necessary to assess potential gastrointestinal irritation.

Nanocapsules

The nanocapsules comprise a polymeric shell that encapsulates a drug-loaded core,[135] as summarized in Table 5. In a study conducted by AbdElhamid et al, CXB and HNK co-loaded quantum dots-based nanocapsules were developed and modified with CS and Lf (C/H-Lf-QDs-CS-NCs) for targeted therapy and imaging of breast cancer.[127] The studies revealed that the tumor volume increased by 172.30% in the free CXB/HNK group, whereas it only increased by 48.12% in the C/H-Lf-QDs-CS-NCs group, demonstrating enhanced antitumor efficacy. Moreover, the mice treated with C/H-Lf-QDs-CS-NCs exhibited distinct fluorescence in the tumor tissue at a wavelength of 450 nm, indicating their imaging capability. In another study by Haggag et al, a novel formulation of PEGylated PLGA nanocapsules loaded with HNK was prepared.[128] These nanocapsules exhibited remarkable inhibition rates of 80.2% and 58.1% on MCF-7 and EAC cells, respectively. In contrast, the inhibition rates of free HNK were 35% and 31%, respectively. Notably, these nanocapsules also demonstrated 2.3 times stronger inhibition of solid Ehrlich tumor growth than free HNK, effectively enhancing the anticancer effect of HNK. Despite the favorable attributes of HNK-loaded nanocapsules, such as high entrapment efficiency, sustained release, and enhanced therapeutic effects, the majority of these studies remain confined to laboratory-scale experiments, and achieving large-scale production remains a challenge.

Dendrimers

Dendrimers possess remarkable drug-loading capabilities due to their abundant surface functional groups and internal cavities. This unique property allows for both covalent and non-covalent interactions with drugs, thereby enhancing their bioavailability.[136] The two primary types of dendrimers currently utilized for HNK loading are PAMAM and triazine-based dendrimers, as detailed in Table 5.

One study employed PAMAM G4.0 dendrimers and fluorescent-labeled amphiphilic copolymer PGC as carriers for HNK encapsulation (HK NPs).[129] Remarkably, the drug loading capacity of HK NPs reached up to 60%, with a sustained release of HNK over 120 hours. The uptake of HK NPs in 4T1 cells was found to be 10-fold higher than free HNK, resulting in significantly enhanced cytotoxicity and antitumor activity. To address early caries lesions in enamel, HNK-loaded PAMAM dendrimers (PAMH) were developed.[32] PAMH displayed a slower but more persistent release of HNK under cariogenic pH environments compared to neutral pH, achieving a long-lasting antimicrobial effect. The PAMH group exhibited higher mineral density in the rat's molar area and a larger residual enamel volume than the PAMAM or control group, indicating effective resistance to caries lesions. Additionally, Khalil et al synthesized an s-triazine-based dendrimer conjugated with HNK, which was further modified with FA or lactic acid for targeted delivery to hepatocellular carcinoma cells.[130] To enhance the pharmacokinetics, the dendrimer conjugate was PEGylated. Notably, the resulting conjugate demonstrated a targeted inhibitory effect on matrix metalloproteinase-2/9, leading to enhanced cytotoxicity against liver cancer cells. However, the cytotoxicity associated with dendrimers is a concern that needs attention and is a significant factor limiting their medical applications.

Nanosuspensions

Nanosuspensions, characterized as submicron two-phase colloidal dispersions consisting of pure drugs and small amounts of surfactants or polymeric materials, offer a promising approach for delivering hydrophobic drugs.[137]

Han et al employed the solvent precipitation-ultrasound method to prepare HNK nanosuspensions, using BSA and PVP as stabilizers (Table 5).[131] The resulting nanosuspensions exhibited about 3.94 and 2.2 times higher C_{max} and $AUC_{(0-t)}$ values than free HNK, significantly enhancing HNK's oral bioavailability. After intraperitoneal administration, the distribution of HNK nanosuspensions was increased in the blood, heart, and brain, offering potential therapeutic benefits for cardiovascular diseases. In a separate investigation, Lu and coworkers prepared HNK nanosuspensions (HNS) to improve the dissolution rate of HNK.[132] In a mouse ear swelling model induced by xylene, the swelling inhibition rate in the HNS treatment group was 1.7 times higher compared to free HNK, significantly enhancing the anti-

inflammatory effect of HNK. Despite the advantageous impact of nanosuspension on enhancing the water solubility and efficacy of HNK, the stability of these nanosuspensions remains an aspect requiring further improvement.

Nanofibers

Electrospun nanofibers are continuous nanofibrous structures derived from polymer solutions through high-voltage electrostatics, resulting in adjustable submicron structures capable of loading and controlling the release of drugs. Researchers successfully prepared an electrospun nanofiber incorporating HNK using PLGA copolymer as a carrier (Table 5).[133] This system exhibited controlled release of HNK over 24 hours and effectively inhibited the proliferation and migration of kidney cancer cells, but further in vivo studies are required to verify the potential of nanofibers as sustained release carriers.

Nanodroplets

Nanodroplets are composed of a perfluorinated carbon core enveloped by a stable lipid shell. The core remains in a liquid state at body temperature but converts into microbubbles upon exposure to ultrasound, thus facilitating the extravasation of drugs into target tissues.[138] Zhang et al developed HNK-encapsulated nanodroplets, further modified with GA to enhance their targeting ability, with a particle size of about 324.8 nm (Table 5).[134] Due to GA receptor-mediated endocytosis, the uptake of nanodroplets in HepG2 cells was significantly increased, thereby augmenting the cytotoxicity. Moreover, the antitumor effect of nanodroplets was markedly enhanced in HepG2 tumor-bearing mice. Notably, the nanodroplets displayed hyperechoic regions under the acoustic droplet evaporation technique, enabling real-time monitoring through ultrasound imaging. However, achieving nanodroplets with a smaller particle size and improved stability is an area requiring further research.

Discussion and Perspectives

In recent decades, natural compounds such as HNK have emerged as an essential source of novel pharmaceuticals, attracting considerable attention due to their multiple pharmacological activities. Nevertheless, the inherent limitations of HNK, including low solubility, poor bioavailability, and rapid metabolism, necessitate the development of NDDSs to enhance its therapeutic efficacy. This review highlights the effectiveness of HNK-loaded nano-formulations in improving solubility, bioavailability, and in vivo circulation time.[80,130] Furthermore, the review summarizes studies that explore the combination of HNK nano-formulations with other drugs or the co-delivery of dual drugs to enhance efficacy and reduce side effects. For instance, the co-administration of HNK liposomes with DOX or DDP has demonstrated enhanced anticancer effect,[41,50] and the co-encapsulation of PTX and HNK within micelles effectively suppresses drug resistance and metastasis in breast cancer.[29] Additionally, researchers have successfully modified NDDSs loaded with HNK using HA, FA, Lf, or other ligands to facilitate targeted delivery, thereby enhancing drug selectivity and therapeutic efficiency.[46,81,83,127] Moreover, the design of carriers employing metals, DMXAA, PBAE, PNIPAM, and other stimuli-responsive materials allows for the controlled release of HNK under specific environments, thereby improving therapeutic effects.[33,79,80,84,119]

The majority of HNK nano-formulations have been primarily studied for their potential to enhance the therapeutic effects in various types of tumors, with a predominant focus on breast,[30,44,84,118] lung,[45,71,112] and liver cancers,[37,109] as illustrated in Figure 3. Also, HNK-loaded nano-formulations have demonstrated promising applications in diverse areas, including but not limited to enhancing anti-caries effects,[32] addressing age-related macular degeneration,[94] showing anti-inflammation ability,[132] exhibiting antibacterial properties,[70] and providing treatment for Alzheimer's disease.[125] In addition, the delivery of HNK through nanocarriers holds therapeutic potential for cardiovascular diseases,[131] such as protection against ischemia-reperfusion injury in the rat brain.[80] Nevertheless, the exploration of HNK nano-formulations in cardiovascular and neurological fields appears to be insufficient and deserves more attention in future research endeavors.

Looking forward, the development of NDDSs for HNK holds immense potential for clinical applications. However, several challenges in the field still need to be solved. One such challenge involves enhancing the safety profiles of nanocarriers employed for HNK delivery. Currently, numerous green synthesis methods have been reported, offering the potential to prepare safer and more effective nano-preparations. This avenue represents a promising direction for the

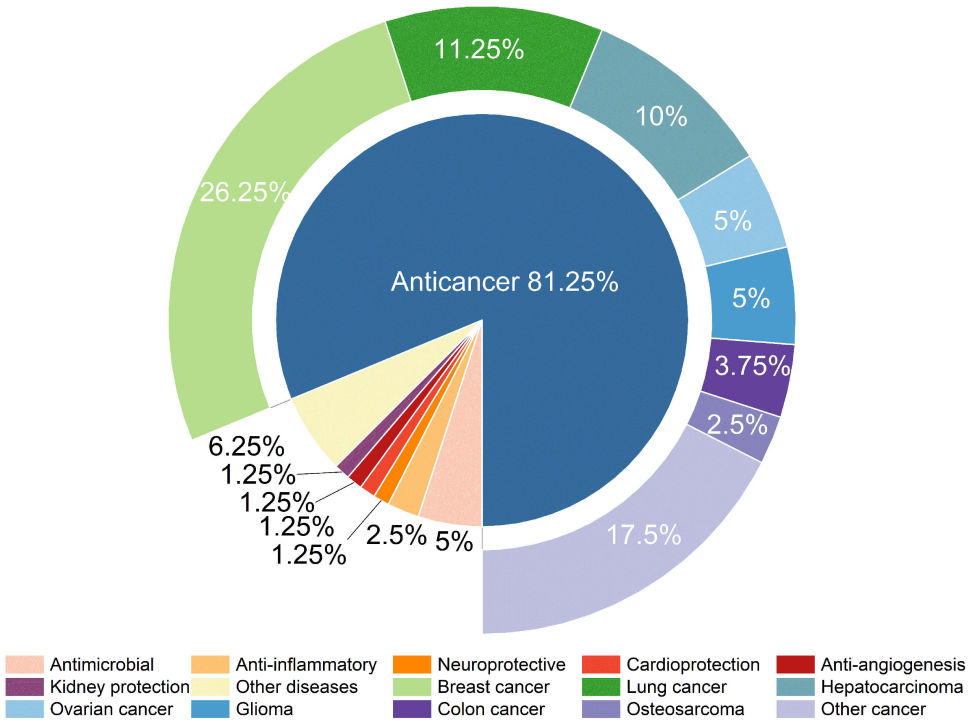

Figure 3 Therapeutic application of nano-formulation loaded with HNK.

future development of HNK delivery systems.[139–143] While there exists a variety of delivery systems for HNK, detailed characterizations of many nano-formulations, such as particle size, zeta potential, drug loading rates, and stability, often remain unexplored. Furthermore, some studies lack in-depth investigations into the in vivo effects of NDDSs, which are essential for verifying whether the outcomes align with those observed in vitro experiments. Future research should focus on optimizing the formulation and manufacturing processes of these nanocarriers to ensure reproducibility, scalability, and cost-effectiveness. Additionally, more studies are needed to evaluate the long-term safety, biocompatibility, and pharmacokinetics of these nano-formulations in preclinical and clinical settings. Furthermore, the integration of HNK-loaded nano-formulations with other therapeutic modalities, such as photothermal therapy, photodynamic therapy, or immunotherapy, should be explored to harness synergistic effects and improve treatment outcomes. The use of targeted delivery strategies, such as surface modifications with ligands or antibodies, can enhance the accumulation of HNK at the site of action, minimizing off-target effects and improving therapeutic selectivity. Addressing these challenges with advancements in science and technology will offer hope for the clinical translation of HNK's nano-delivery systems.

Conclusions

In summary, NDDSs have emerged as promising approaches to overcome the limitations of HNK and enhance its therapeutic potential. These nano-formulations have effectively improved the solubility and bioavailability of HNK, enabling targeted delivery and sustained release. As a result, they have demonstrated enhanced therapeutic efficacy in a wide range of diseases, including cancer, inflammation, bacterial infections, and neurological disorders. However, addressing the remaining challenges will be crucial for the successful clinical translation of HNK nano-formulations.

Author Contributions

All authors made a significant contribution to the work reported, whether in the conception, study design, execution, acquisition of data, analysis, and interpretation, or in all these areas, took part in drafting, revising, or critically reviewing the article; gave final approval of the version to be published; have agreed on the journal to which the article has been submitted; and agree to be accountable for all aspects of the work.

Funding

The National Natural Science Foundation of China (82104083) provided support for this research project.

Disclosure

The authors declare that the research was conducted without any commercial or financial relationships that could be construed as a potential conflict of interest.

References

1. Arora S, Singh S, Piazza GA, Contreras CM, Panyam J, Singh AP. Honokiol: a novel natural agent for cancer prevention and therapy. *Curr Mol Med*. 2012;12(10):1244–1252. doi:10.2174/156652412803833508
2. Sarrica A, Kirika N, Romeo M, Salmona M, Diomede L. Safety and toxicology of magnolol and honokiol. *Planta Med*. 2018;84(16):1151–1164. doi:10.1055/a-0642-1966
3. Rauf A, Patel S, Imran M, et al. Honokiol: an anticancer lignan. *Biomed Pharmacother*. 2018;107:555–562. doi:10.1016/j.biopha.2018.08.054
4. Wang D, Cao L, Zhou X, et al. Mitigation of honokiol on fluoride-induced mitochondrial oxidative stress, mitochondrial dysfunction, and cognitive deficits through activating AMPK/PGC-1α/Sirt3. *J Hazard Mater*. 2022;437:129381. doi:10.1016/j.jhazmat.2022.129381
5. Tang P, Gu JM, Xie ZA, et al. Honokiol alleviates the degeneration of intervertebral disc via suppressing the activation of TXNIP-NLRP3 inflammasome signal pathway. *Free Radic Biol Med*. 2018;120:368–379. doi:10.1016/j.freeradbiomed.2018.04.008
6. Ma D, Cui X, Zhang Z, et al. Honokiol suppresses mycelial growth and reduces virulence of *Botrytis cinerea* by inducing autophagic activities and apoptosis. *Food Microbiol*. 2020;88:103411. doi:10.1016/j.fm.2019.103411
7. Kim H, Lim CY, Chung MS. *Magnolia officinalis* and its honokiol and magnolol constituents inhibit human norovirus surrogates. *Foodborne Pathog Dis*. 2021;18(1):24–30. doi:10.1089/fpd.2020.2805
8. Ding Y, Song Z, Li H, et al. Honokiol ameliorates high-fat-diet-induced obesity of different sexes of mice by modulating the composition of the gut microbiota. *Front Immunol*. 2019;10:2800. doi:10.3389/fimmu.2019.02800
9. Jayakumari NR, Rajendran RS, Sivasailam A, et al. Honokiol regulates mitochondrial substrate utilization and cellular fatty acid metabolism in diabetic mice heart. *Eur J Pharmacol*. 2021;896:173918. doi:10.1016/j.ejphar.2021.173918
10. Lee IH, Im E, Lee H-J, et al. Apoptotic and antihepatofibrotic effect of honokiol via activation of GSK3β and suppression of Wnt/β-catenin pathway in hepatic stellate cells. *Phytother Res*. 2021;35(1):452–462. doi:10.1002/ptr.6824
11. Dai X, Xie L, Liu K, et al. The neuropharmacological effects of magnolol and honokiol: a review of signal pathways and molecular mechanisms. *Curr Mol Pharmacol*. 2023;16:161–177. doi:10.2174/1874467215666220223141101
12. Kim YJ, Jung UJ. Honokiol improves insulin resistance, hepatic steatosis, and inflammation in type 2 diabetic *db/db* mice. *Int J Mol Sci*. 2019;20(9):2303. doi:10.3390/ijms20092303
13. Ding Y, Zhang L, Yao X, et al. Honokiol alleviates high-fat diet-induced obesity of mice by inhibiting adipogenesis and promoting white adipose tissue browning. *Animals*. 2021;11(6):1493. doi:10.3390/ani11061493
14. Rauf A, Olatunde A, Imran M, et al. Honokiol: a review of its pharmacological potential and therapeutic insights. *Phytomedicine*. 2021;90:153647. doi:10.1016/j.phymed.2021.153647
15. Ong CP, Lee WL, Tang YQ, Yap WH. Honokiol: a review of its anticancer potential and mechanisms. *Cancers*. 2020;12(1):48. doi:10.3390/cancers12010048
16. Halasi M, Hitchinson B, Shah BN, et al. Honokiol is a FOXM1 antagonist. *Cell Death Dis*. 2018;9(2):84. doi:10.1038/s41419-017-0156-7
17. Ji H, Wang W, Li X, et al. Natural small molecules enabled efficient immunotherapy through supramolecular self-assembly in p53-mutated colorectal cancer. *Acs Appl Mater Interfaces*. 2022;14(2):2464–2477. doi:10.1021/acsami.1c16737
18. Khatoon F, Ali S, Kumar V, et al. Pharmacological features, health benefits and clinical implications of honokiol. *J Biomol Struct Dyn*. 2023;41(15) :7511–7533. doi:10.1080/07391102.2022.2120541
19. Sheng YL, Xu JH, Shi CH, et al. UPLC-MS/MS-ESI assay for simultaneous determination of magnolol and honokiol in rat plasma: application to pharmacokinetic study after administration emulsion of the isomer. *J Ethnopharmacol*. 2014;155(3):1568–1574. doi:10.1016/j.jep.2014.07.052
20. Nasibova A. Generation of nanoparticles in biological systems and their application prospects. *Advances in Biology & Earth Sciences*. 2023;8(2):140–146.
21. Eftekhari A, Kryschi C, Pamies D, et al. Natural and synthetic nanovectors for cancer therapy. *Nanotheranostics*. 2023;7(3):236–257. doi:10.7150/ntno.77564
22. Abdullah, Al-Radadi NS, Hussain T, Faisal S, Ali Raza Shah S. Novel biosynthesis, characterization and bio-catalytic potential of green algae (*Spirogyra hyalina*) mediated silver nanomaterials. *Saudi J Biol Sci*. 2022;29(1):411–419. doi:10.1016/j.sjbs.2021.09.013
23. Jain S, Dongare K, Nallamothu B, et al. Enhanced stability and oral bioavailability of erlotinib by solid self nano emulsifying drug delivery systems. *Int J Pharm*. 2022;622:121852. doi:10.1016/j.ijpharm.2022.121852
24. Raza A, Hayat U, Rasheed T, Bilal M, Iqbal HMN. Redox-responsive nano-carriers as tumor-targeted drug delivery systems. *Eur J Med Chem*. 2018;157:705–715. doi:10.1016/j.ejmech.2018.08.034
25. Shi Y, van der Meel R, Chen X, Lammers T. The EPR effect and beyond: strategies to improve tumor targeting and cancer nanomedicine treatment efficacy. *Theranostics*. 2020;10(17):7921–7924. doi:10.7150/thno.49577
26. Srinivasarao M, Low PS. Ligand-targeted drug delivery. *Chem Rev*. 2017;117(19):12133–12164. doi:10.1021/acs.chemrev.7b00013
27. Zheng Z, Zhang J, Jiang J, et al. Remodeling tumor immune microenvironment (TIME) for glioma therapy using multi-targeting liposomal codelivery. *J Immunother Cancer*. 2020;8(2):e000207. doi:10.1136/jitc-2019-000207

28. He Y, Wan J, Yang Y, et al. M Multifunctional polypyrrole-coated mesoporous TiO_2 nanocomposites for photothermal, sonodynamic, and chemotherapeutic treatments and dual-modal ultrasound/photoacoustic imaging of tumors. *Adv Healthc Mater*. 2019;8(9):e1801254. doi:10.1002/adhm.201801254
29. Wang N, Wang Z, Nie S, et al. Biodegradable polymeric micelles coencapsulating paclitaxel and honokiol: a strategy for breast cancer therapy in vitro and in vivo. *Int J Nanomedicine*. 2017;12:1499–1514. doi:10.2147/ijn.S124843
30. Atallah MA, Sallam MA, Abdelmoneem MA, et al. Green self-assembled lactoferrin carboxymethyl cellulose nanogels for synergistic chemo/herbal breast cancer therapy. *Colloids Surf B Biointerfaces*. 2022;217:112657. doi:10.1016/j.colsurfb.2022.112657
31. Ding W, Hou X, Cong S, et al. Co-delivery of honokiol, a constituent of magnolia species, in a self-microemulsifying drug delivery system for improved oral transport of lipophilic sirolimus. *Drug Deliv*. 2016;23(7):2513–2523. doi:10.3109/10717544.2015.1020119
32. Tao S, Yang X, Liao L, et al. A novel anticaries agent, honokiol-loaded poly(amido amine) dendrimer, for simultaneous long-term antibacterial treatment and remineralization of demineralized enamel. *Dent Mater*. 2021;37(9):1337–1349. doi:10.1016/j.dental.2021.06.003
33. Liu Z, Tang Z, Zhang D, et al. A novel GSH responsive poly(alpha-lipoic acid) nanocarrier bonding with the honokiol-DMXAA conjugate for combination therapy. *Sci China Mater*. 2020;63(2):307–315. doi:10.1007/s40843-019-1183-0
34. Agarwal S, Muniyandi P, Maekawa T, Kumar DS. Vesicular systems employing natural substances as promising drug candidates for MMP inhibition in glioblastoma: a nanotechnological approach. *Int J Pharm*. 2018;551(1–2):339–361. doi:10.1016/j.ijpharm.2018.09.033
35. Wang XH, Cai LL, Zhang XY, et al. Improved solubility and pharmacokinetics of PEGylated liposomal honokiol and human plasma protein binding ability of honokiol. *Int J Pharm*. 2011;410(1–2):169–174. doi:10.1016/j.ijpharm.2011.03.003
36. Yang J, Wu W, Wen J, et al. Liposomal honokiol induced lysosomal degradation of Hsp90 client proteins and protective autophagy in both gefitinib-sensitive and gefitinib-resistant NSCLC cells. *Biomaterials*. 2017;141:188–198. doi:10.1016/j.biomaterials.2017.07.002
37. Wang X, Deng L, Cai L, et al. Preparation, characterization, pharmacokinetics, and bioactivity of honokiol-in-hydroxypropyl-β-cyclodextrin-in-liposome. *J Pharm Sci*. 2011;100(8):3357–3364. doi:10.1002/jps.22534
38. Luo H, Zhong Q, Chen LJ, et al. Liposomal honokiol, a promising agent for treatment of cisplatin-resistant human ovarian cancer. *J Cancer Res Clin Oncol*. 2008;134(9):937–945. doi:10.1007/s00432-008-0375-5
39. Wen J, Fu AF, Chen LJ, et al. Liposomal honokiol inhibits VEGF-D-induced lymphangiogenesis and metastasis in xenograft tumor model. *Int J Cancer*. 2009;124(11):2709–2718. doi:10.1002/ijc.24244
40. Zhou C, Guo C, Li W, et al. A novel honokiol liposome: formulation, pharmacokinetics, and antitumor studies. *Drug Dev Ind Pharm*. 2018;44(12):2005–2012. doi:10.1080/03639045.2018.1506475
41. Liu Y, Chen L, He X, et al. Enhancement of therapeutic effectiveness by combining liposomal honokiol with cisplatin in ovarian carcinoma. *Int J Gynecol Cancer*. 2008;18(4):652–659. doi:10.1111/j.1525-1438.2007.01070.x
42. Jiang QQ, Fan LY, Yang GL, et al. Improved therapeutic effectiveness by combining liposomal honokiol with cisplatin in lung cancer model. *BMC Cancer*. 2008;8:242. doi:10.1186/1471-2407-8-242
43. Cheng N, Xia T, Han Y, He QJ, Zhao R, Ma JR. Synergistic antitumor effects of liposomal honokiol combined with cisplatin in colon cancer models. *Oncol Lett*. 2011;2(5):957–962. doi:10.3892/ol.2011.350
44. Hou W, Chen L, Yang G, et al. Synergistic antitumor effects of liposomal honokiol combined with adriamycin in breast cancer models. *Phytother Res*. 2008;22(8):1125–1132. doi:10.1002/ptr.2472
45. Jin X, Yang Q, Cai N, Zhang Z. A cocktail of betulinic acid, parthenolide, honokiol and ginsenoside Rh2 in liposome systems for lung cancer treatment. *Nanomedicine*. 2020;15(1):41–54. doi:10.2217/nnm-2018-0479
46. Wang J, Liu D, Guan S, et al. Hyaluronic acid-modified liposomal honokiol nanocarrier: enhance anti-metastasis and antitumor efficacy against breast cancer. *Carbohydr Polym*. 2020;235:115981. doi:10.1016/j.carbpol.2020.115981
47. Zhang X, Chen H, Zhang Y, et al. HA-DOPE-modified honokiol-loaded liposomes targeted therapy for osteosarcoma. *Int J Nanomedicine*. 2022;17:5137–5151. doi:10.2147/ijn.s371934
48. Li X, Guan S, Li H, et al. Polysialic acid-functionalized liposomes for efficient honokiol delivery to inhibit breast cancer growth and metastasis. *Drug Deliv*. 2023;30(1):2181746. doi:10.1080/10717544.2023.2181746
49. Liu S, Zhang S, Ju R, et al. Antitumor efficacy of Lf modified daunorubicin plus honokiol liposomes in treatment of brain glioma. *Eur J Pharm Sci*. 2017;106:185–197. doi:10.1016/j.ejps.2017.06.002
50. Song X, Ju R, Xiao Y, et al. Application of multifunctional targeting epirubicin liposomes in the treatment of non-small-cell lung cancer. *Int J Nanmedicine*. 2017;12:7433–7451. doi:10.2147/ijn.S141787
51. Ju R, Cheng L, Qiu X, et al. Hyaluronic acid modified daunorubicin plus honokiol cationic liposomes for the treatment of breast cancer along with the elimination vasculogenic mimicry channels. *J Drug Target*. 2018;26(9):793–805. doi:10.1080/1061186x.2018.1428809
52. Hsiao Y, Chen H, Liang Y, et al. Development of nanosome-encapsulated honokiol for intravenous therapy against experimental autoimmune encephalomyelitis. *Int J Nanomedicine*. 2020;15:17–29. doi:10.2147/ijn.S214349
53. Kanchanapally R, Khan MA, Deshmukh SK, et al. Exosomal formulation escalates cellular uptake of honokiol leading to the enhancement of its antitumor efficacy. *Acs Omega*. 2020;5(36):23299–23307. doi:10.1021/acsomega.0c03136
54. Ezzeldeen Y, Swidan S, ElMeshad A, Sebak A. Green synthesized honokiol transfersomes relieve the immunosuppressive and stem-like cell characteristics of the aggressive B16F10 melanoma. *Int J Nanomedicine*. 2021;16:5693–5712. doi:10.2147/ijn.S314472
55. Dymek M, Sikora E. Liposomes as biocompatible and smart delivery systems - the current state. *Adv Colloid Interface Sci*. 2022;309:102757. doi:10.1016/j.cis.2022.102757
56. Li S, Li L, Chen J, et al. Liposomal honokiol inhibits glioblastoma growth through regulating macrophage polarization. *Ann Transl Med*. 2021;9(22):1644. doi:10.21037/atm-21-1836
57. Li S, Chen J, Fan Y, et al. Liposomal Honokiol induces ROS-mediated apoptosis via regulation of ERK/p38-MAPK signaling and autophagic inhibition in human medulloblastoma. *Signal Transdu Target Ther*. 2022;7(1):49. doi:10.1038/s41392-021-00869-w
58. Abu Lila AS, Ishida T. Liposomal delivery systems: design optimization and current applications. *Biol Pharm Bull*. 2017;40(1):1–10. doi:10.1248/bpb.b16-00624
59. Kundu AK, Hazari S, Chinta DD, Pramar YV, Dash S, Mandal TK. Development of nanosomes using high-pressure homogenization for gene therapy. *J Pharm Pharmacol*. 2010;62(9):1103–1111. doi:10.1111/j.2042-7158.2010.01140.x

60. Liu H, Wang T, Hsu Y, et al. Nanoparticulated honokiol mitigates cisplatin-induced chronic kidney injury by maintaining mitochondria antioxidant capacity and reducing caspase 3-associated cellular apoptosis. *Antioxidants*. 2019;8(10):466. doi:10.3390/antiox8100466
61. Wang T, Lai Y, Yang K, Lin S, Chen C, Tsai P. Counteracting cisplatin-induced testicular damages by natural polyphenol constituent honokiol. *Antioxidants*. 2020;9(8):723. doi:10.3390/antiox9080723
62. Kalluri R, LeBleu VS. The biology, function, and biomedical applications of exosomes. *Science*. 2020;367(6478):aau6977. doi:10.1126/science.aau6977
63. Liang Y, Duan L, Lu J, Xia J. Engineering exosomes for targeted drug delivery. *Theranostics*. 2021;11(7):3183–3195. doi:10.7150/thno.52570
64. Gupta R, Kumar A. Transfersomes: the ultra-deformable carrier system for non-invasive delivery of drug. *Curr Drug Deliv*. 2021;18(4):408–420. doi:10.2174/1567201817666200804105416
65. Khizar S, Alrushaid N, Alam Khan F, et al. Nanocarrier based novel and effective drug delivery system. *Int J Pharm*. 2022;632:122570. doi:10.1016/j.ijpharm.2022.122570
66. Gou ML, Dai M, Li XY, et al. Preparation and characterization of honokiol nanoparticles. *J Mater Sci Mater Med*. 2008;19(7):2605–2608. doi:10.1007/s10856-007-3361-6
67. Wu W, Wang L, Wang L, et al. Preparation of honokiol nanoparticles by liquid antisolvent precipitation technique, characterization, pharmacokinetics, and evaluation of inhibitory effect on HepG2 cells. *Int J Nanomedicine*. 2018;13:5469–5483. doi:10.2147/ijn.S178416
68. Gou M, Zheng L, Peng X, et al. Poly(ε-caprolactone)-poly(ethylene glycol) -poly(ε-caprolactone) (PCL-PEG-PCL) nanoparticles for honokiol delivery *in vitro*. *Int J Pharm*. 2009;375(1–2):170–176. doi:10.1016/j.ijpharm.2009.04.007
69. Zheng X, Kan B, Gou M, et al. Preparation of MPEG-PLA nanoparticle for honokiol delivery *in vitro*. *Int J Pharm*. 2010;386(1–2):262–267. doi:10.1016/j.ijpharm.2009.11.014
70. Wang Y, Ding C, Ge Z, et al. A novel antibacterial and fluorescent coating composed of polydopamine and carbon dots on the surface of orthodontic brackets. *J Mater Sci Mater Med*. 2023;34(2):10. doi:10.1007/s10856-023-06712-8
71. Tang P, Sun Q, Yang H, Tang B, Pu H, Li H. Honokiol nanoparticles based on epigallocatechin gallate functionalized chitin to enhance therapeutic effects against liver cancer. *Int J Pharm*. 2018;545(1–2):74–83. doi:10.1016/j.ijpharm.2018.04.060
72. He Y, Hou X, Guo J, et al. Activation of a gamma-cyclodextrin-based metal-organic framework using supercritical carbon dioxide for high-efficient delivery of honokiol. *Carbohydr Polym*. 2020;235:115935. doi:10.1016/j.carbpol.2020.115935
73. Deng F, Hu W, Chen H, Tang Y, Zhang L. Development of a chitosan-based nanoparticle formulation for ophthalmic delivery of honokiol. *Curr Drug Deliv*. 2018;15(4):594–600. doi:10.2174/1567201814666170419113933
74. Weng Y, Zhang H, Xu S, et al. Preparation and quality evaluation of honokiol nanoparticles using a new polysaccharide polymer as its carrier. *Curr Drug Deliv*. 2023;20(2):183–191. doi:10.2174/1567201819666220607153457
75. Dong Z, Qiu H, Han M, Wang R, Guo Y, Wang X. Honokiol-based nanomedicine decorated with ethylene glycols derivatives promotes antitumor efficacy. *J Biomed Nanotechnol*. 2021;17(8):1564–1573. doi:10.1166/jbn.2021.3126
76. Zhang Y, Chen T, Yuan P, et al. Encapsulation of honokiol into self-assembled pectin nanoparticles for drug delivery to HepG2 cells. *Carbohydr Polym*. 2015;133:31–38. doi:10.1016/j.carbpol.2015.06.102
77. Yang B, Ni X, Chen L, et al. Honokiol-loaded polymeric nanoparticles: an active targeting drug delivery system for the treatment of nasopharyngeal carcinoma. *Drug Deliv*. 2017;24(1):660–669. doi:10.1080/10717544.2017.1303854
78. Salah M, Sallam MA, Abdelmoneem MA, et al. Sequential delivery of novel triple drug combination via crosslinked alginate/lactoferrin nanohybrids for enhanced breast cancer treatment. *Pharmaceutics*. 2022;14(11):2404. doi:10.3390/pharmaceutics14112404
79. Zhang H, Li J, Yuan R, et al. Augment the efficacy of eradicating metastatic lesions and tumor proliferation in breast cancer by honokiol-loaded pH-sensitive targeted lipid nanoparticles. *Colloids Surf B Biointerfaces*. 2021;207:112008. doi:10.1016/j.colsurfb.2021.112008
80. Wei X, Fang Z, Sheng J, Wang Y, Lu P. Honokiol-mesoporous silica nanoparticles inhibit vascular restenosis via the suppression of TGF-β signaling pathway. *Int J Nanomedicine*. 2020;15:5239–5252. doi:10.2147/ijn.S250911
81. Deb A, Andrews NG, Raghavan V. Honokiol-camptothecin loaded graphene oxide nanoparticle towards combinatorial anti-cancer drug delivery. *IET Nanobiotechnol*. 2020;14(9):796–802. doi:10.1049/iet-nbt.2020.0103
82. Zhang Q, Wang J, Liu D, et al. Targeted delivery of honokiol by zein/hyaluronic acid core-shell nanoparticles to suppress breast cancer growth and metastasis. *Carbohydr Polym*. 2020;240:116325. doi:10.1016/j.carbpol.2020.116325
83. Zhang Q, Li D, Guan S, et al. Tumor-targeted delivery of honokiol via polysialic acid modified zein nanoparticles prevents breast cancer progression and metastasis. *Int J Biol Macromol*. 2022;203:280–291. doi:10.1016/j.ijbiomac.2022.01.148
84. Yu R, Zou Y, Liu B, Guo Y, Wang X, Han M. Surface modification of pH-sensitive honokiol nanoparticles based on dopamine coating for targeted therapy of breast cancer. *Colloids Surf B Biointerfaces*. 2019;177:1–10. doi:10.1016/j.colsurfb.2019.01.047
85. Chen L, Li S, Ding Y, et al. Honokiol prodrug nanoparticles based on in situ albumin binding for long circulation and high tumor uptake. *Acs Med Chem Lett*. 2021;12(10):1589–1595. doi:10.1021/acsmedchemlett.1c00429
86. Dai T, He W, Yao C, et al. Applications of inorganic nanoparticles in the diagnosis and therapy of atherosclerosis. *Biomater Sci*. 2020;8(14):3784–3799. doi:10.1039/d0bm00196a
87. Faisal S, Jan H, Abdullah, et al. In vivo analgesic, anti-inflammatory, and anti-diabetic screening of *bacopa monnieri*-synthesized copper oxide nanoparticles. *ACS Omega*. 2022;7(5):4071–4082. doi:10.1021/acsomega.1c05410
88. Kainat, Khan MA, Ali F, et al. Exploring the therapeutic potential of *Hibiscus Rosa sinensis* synthesized cobalt oxide (Co_3O_4-NPs) and magnesium oxide nanoparticles (MgO-NPs). *Saudi J Biol Sci*. 2021;28(9):5157–5167. doi:10.1016/j.sjbs.2021.05.035
89. Jan H, Khan MA, Usman H, et al. The *Aquilegia pubiflora* (Himalayan columbine) mediated synthesis of nanoceria for diverse biomedical applications. *RSC Adv*. 2020;10(33):19219–19231. doi:10.1039/d0ra01971b
90. Faisal S, Jan H, Shah SA, et al. Green synthesis of zinc oxide (ZnO) nanoparticles using aqueous fruit extracts of *Myristica fragrans*: their characterizations and biological and environmental applications. *ACS Omega*. 2021;6(14):9709–9722. doi:10.1021/acsomega.1c00310
91. Faisal S, Khan MA, Jan H, et al. Edible mushroom (*Flammulina velutipes*) as biosource for silver nanoparticles: from synthesis to diverse biomedical and environmental applications. *Nanotechnology*. 2021;32(6):065101. doi:10.1088/1361-6528/abc2eb
92. Ghezzi M, Pescina S, Padula C, et al. Polymeric micelles in drug delivery: an insight of the techniques for their characterization and assessment in biorelevant conditions. *J Control Release*. 2021;332:312–336. doi:10.1016/j.jconrel.2021.02.031

93. Gou M, Zheng X, Men K, et al. Self-assembled hydrophobic honokiol loaded MPEG-PCL diblock copolymer micelles. *Pharm Res*. 2009;26(9):2164–2173. doi:10.1007/s11095-009-9929-8
94. Shahid A, Bhatt P, Miller A, Sutariya V. Honokiol-loaded methoxy poly (ethylene glycol) polycaprolactone micelles for the treatment of age-related macular degeneration. *Assay Drug Dev Technol*. 2021;19(6):350–360. doi:10.1089/adt.2021.003
95. Cheng Y, Zheng S, Teng Y, et al. Preparation of honokiol with biodegradable nanoparticles for treatment of osteosarcoma. *RSC Adv*. 2016;6(96):94278–94286. doi:10.1039/c6ra21479g
96. Gao X, Yu T, Xu G, et al. Enhancing the anti-glioma therapy of doxorubicin by honokiol with biodegradable self-assembling micelles through multiple evaluations. *Sci Rep*. 2017;7:45301. doi:10.1038/srep43501
97. Li X, Hou X, Ding W, et al. Sirolimus-loaded polymeric micelles with honokiol for oral delivery. *J Pharm Pharmacol*. 2015;67(12):1663–1672. doi:10.1111/jphp.12482
98. Sun J, Li J, Liu Q, et al. Tuning mPEG-PLA/vitamin E-TPGS-based mixed micelles for combined celecoxib/honokiol therapy for breast cancer. *Eur J Pharm Sci*. 2020;146:105277. doi:10.1016/j.ejps.2020.105277
99. Wang Z, Li X, Wang D, et al. Concurrently suppressing multidrug resistance and metastasis of breast cancer by co-delivery of paclitaxel and honokiol with pH-sensitive polymeric micelles. *Acta Biomater*. 2017;62:144–156. doi:10.1016/j.actbio.2017.08.027
100. Zou Y, Zhou Y, Jin Y, et al. Synergistically enhanced antimetastasis effects by honokiol-loaded pH-sensitive polymer–doxorubicin conjugate micelles. *Acs Appl Mater Interfaces*. 2018;10(22):18585–18600. doi:10.1021/acsami.8b04854
101. Feng R, Deng P, Zhou F, Feng S, and Song Z. Pluronic F_{127}-cyclodextrin conjugate micelles for encapsulation of honokiol. *Journal of Nanoparticle Research*. 2018;20(10):261. doi:10.1007/s11051-018-4367-3
102. Song Z, Sun J, Deng P, et al. Oligochitosan-pluronic 127 conjugate for delivery of honokiol. *Artif Cells Nanomed Biotechnol*. 2018;46(sup1):740–750. doi:10.1080/21691401.2018.1434785
103. Zhu L, Song Z, Feng S, Xu H, Chen S, Feng R. Biotin-modified oligochitosan-F_{127} micelles for honokiol's encapsulation. *J Nanopart Res*. 2021;23(5):116. doi:10.1007/s11051-021-05229-x
104. Gong C, Wei X, Wang X, et al. Biodegradable self-assembled PEG–PCL–PEG micelles for hydrophobic honokiol delivery: I. Preparation and characterization. *Nanotechnology*. 2010;21(21):215103. doi:10.1088/0957-4484/21/21/215103
105. Wei X, Gong C, Shi S, et al. Self-assembled honokiol-loaded micelles based on poly(ε-caprolactone)-poly(ethylene glycol)-poly(ε-caprolactone) copolymer. *Int J Pharm*. 2009;369(1–2):170–175. doi:10.1016/j.ijpharm.2008.10.027
106. Dong P, Wang X, Gu Y, et al. Self-assembled biodegradable micelles based on star-shaped PCL-*b*-PEG copolymers for chemotherapeutic drug delivery. *Colloids Surf a Physicochem Eng Asp*. 2010;358(1–3):128–134. doi:10.1016/j.colsurfa.2010.01.037
107. Qiu N, Cai L, Xie D, et al. Synthesis, structural and *in vitro* studies of well-dispersed monomethoxy-poly(ethylene glycol)–honokiol conjugate micelles. *Biomed Mater*. 2010;5(6):065006. doi:10.1088/1748-6041/5/6/065006
108. Godugu C, Doddapaneni R, Singh M. Honokiol nanomicellar formulation produced increased oral bioavailability and anticancer effects in triple negative breast cancer (TNBC). *Colloids Surf B Biointerfaces*. 2017;153:208–219. doi:10.1016/j.colsurfb.2017.01.038
109. Wang J, Yang H, Li Q, et al. Novel nanomicelles based on rebaudioside A: a potential nanoplatform for oral delivery of honokiol with enhanced oral bioavailability and antitumor activity. *Int J Pharm*. 2020;590:119899. doi:10.1016/j.ijpharm.2020.119899
110. Zhou L, Wu J, Sun Z, Wang W. Oxidation and reduction dual-responsive polymeric prodrug micelles co-delivery precisely prescribed paclitaxel and honokiol for laryngeal carcinoma combination therapy. *Front Pharmacol*. 2022;13:934632. doi:10.3389/fphar.2022.934632
111. Lin H, Cheng W, Chen L, Ho H, Lin S, Hsieh C. Honokiol/magnolol-loaded self-assembling lecithin-based mixed polymeric micelles (*lb*MPMs) for improving solubility to enhance oral bioavailability. *Int J Nanomedicine*. 2021;16:651–665. doi:10.2147/ijn.S290444
112. Wang X, Cheng L, Xie H, et al. Functional paclitaxel plus honokiol micelles destroying tumour metastasis in treatment of non-small-cell lung cancer. *Artif Cells Nanomed Biotechnol*. 2018;46:1154–1169. doi:10.1080/21691401.2018.1481082
113. Liu X, Li W, Chen T, et al. Hyaluronic acid-modified micelles encapsulating Gem-C_{12} and HNK for glioblastoma multiforme chemotherapy. *Mol Pharm*. 2018;15(3):1203–1214. doi:10.1021/acs.molpharmaceut.7b01035
114. Xu D, Lu Q, Hu X. Down-regulation of P-glycoprotein expression in MDR breast cancer cell MCF-7/ADR by honokiol. *Cancer Lett*. 2006;243(2):274–280. doi:10.1016/j.canlet.2005.11.031
115. Hajebi S, Rabiee N, Bagherzadeh M, et al. Stimulus-responsive polymeric nanogels as smart drug delivery systems. *Acta Biomater*. 2019;92:1–18. doi:10.1016/j.actbio.2019.05.018
116. Fang F, Gong C, Qian Z, et al. Honokiol nanoparticles in thermosensitive hydrogel: therapeutic effects on malignant pleural effusion. *ACS Nano*. 2009;3(12):4080–4088. doi:10.1021/nn900785b
117. Xie Y, Long Q, Wu Q, et al. Improving therapeutic effect in ovarian peritoneal carcinomatosis with honokiol nanoparticles in a thermosensitive hydrogel composite. *RSC Adv*. 2012;2(20):7759–7771. doi:10.1039/c2ra20612a
118. Lu X, Lu X, Yang P, Zhang Z, Lv H. Honokiol nanosuspensions loaded thermosensitive hydrogels as the local delivery system in combination with systemic paclitaxel for synergistic therapy of breast cancer. *Eur J Pharm Sci*. 2022;175:106212. doi:10.1016/j.ejps.2022.106212
119. Metawea ORM, Abdelmoneem MA, Haiba NS, et al. A novel 'smart' PNIPAM-based copolymer for breast cancer targeted therapy: synthesis, and characterization of dual pH/temperature-responsive lactoferrin-targeted PNIPAM-co-AA. *Colloids Surf B Biointerfaces*. 2021;202:111694. doi:10.1016/j.colsurfb.2021.111694
120. Gou M, Li X, Dai M, et al. A novel injectable local hydrophobic drug delivery system: biodegradable nanoparticles in thermo-sensitive hydrogel. *Int J Pharm*. 2008;359(1–2):228–233. doi:10.1016/j.ijpharm.2008.03.023
121. Gou M, Gong C, Zhang J, et al. Polymeric matrix for drug delivery: honokiol-loaded PCL-PEG-PCL nanoparticles in PEG-PCL-PEG thermosensitive hydrogel. *J Biomed Mater Res Part A*. 2010;93A(1):219–226. doi:10.1002/jbm.a.32546
122. Gong CY, Shi S, Dong PW, et al. *In vitro* drug release behavior from a novel thermosensitive composite hydrogel based on Pluronic f127 and poly(ethylene glycol)-poly(ε-caprolactone)-poly(ethylene glycol) copolymer. *BMC Biotechnol*. 2009;9:8. doi:10.1186/1472-6750-9-8
123. Gong C, Shi S, Wang X, et al. Novel composite drug delivery system for honokiol delivery: self-assembled poly(ethylene glycol)-poly(ε-caprolactone)-poly(ethylene glycol) micelles in thermosensitive poly(ethylene glycol)-poly(ε-caprolactone)-poly(ethylene glycol) hydrogel. *J Phys Chem B*. 2009;113(30):10183–10188. doi:10.1021/jp902697d
124. Zheng X, Wang X, Gou M, et al. A novel transdermal honokiol formulation based on Pluronic F127 copolymer. *Drug Deliv*. 2010;17(3):138–144. doi:10.3109/10717541003604874

125. Qu C, Li Q, Su Z, et al. Nano-honokiol ameliorates the cognitive deficits in TgCRND8 mice of Alzheimer's disease via inhibiting neuropathology and modulating gut microbiota. *J Adv Res*. 2022;35:231–243. doi:10.1016/j.jare.2021.03.012
126. Gostynska A, Czerniel J, Kuzminska J, et al. Honokiol-loaded nanoemulsion for glioblastoma treatment: statistical optimization, physicochemical characterization, and an in vitro toxicity assay. *Pharmaceutics*. 2023;15(2):448. doi:10.3390/pharmaceutics15020448
127. AbdElhamid AS, Zayed DG, Helmy MW, et al. Lactoferrin-tagged quantum dots-based theranostic nanocapsules for combined COX-2 inhibitor/herbal therapy of breast cancer. *Nanomedicine*. 2018;13(20):2637–2656. doi:10.2217/nnm-2018-0196
128. Haggag YA, Ibrahim RR, Hafiz AA. Design, formulation and in vivo evaluation of novel honokiol-loaded PEGylated PLGA nanocapsules for treatment of breast cancer. *Int J Nanomedicine*. 2020;15:1625–1642. doi:10.2147/ijn.S241428
129. Guo Y, Zhao Y, Wang T, et al. Honokiol nanoparticles stabilized by oligoethylene glycols codendrimer: *in vitro* and *in vivo* investigations. *J Mater Chem B*. 2017;5(4):697–706. doi:10.1039/c6tb02416e
130. Khalil HH, Osman HA, Teleb M, et al. Engineered s-triazine-based dendrimer-honokiol conjugates as targeted MMP-2/9 inhibitors for halting hepatocellular carcinoma. *ChemMedChem*. 2021;16(24):3701–3719. doi:10.1002/cmdc.202100465
131. Han M, Yu X, Guo Y, Wang Y, Kuang H, Wang X. Honokiol nanosuspensions: preparation, increased oral bioavailability and dramatically enhanced biodistribution in the cardio-cerebro-vascular system. *Colloids Surf B Biointerfaces*. 2014;116:114–120. doi:10.1016/j.colsurfb.2013.12.056
132. Lu X, Lu X, Zhang Z, Lv H. Preparation and characterization of honokiol nanosuspensions and preliminary evaluation of anti-inflammatory effect. *AAPS PharmSciTech*. 2020;21(2):62. doi:10.1208/s12249-019-1602-x
133. Hamedani Y, Chakraborty S, Sabarwal A, Pal S, Bhowmick S, Balan M. Novel honokiol-eluting PLGA-based scaffold effectively restricts the growth of renal cancer cells. *PLoS One*. 2020;15(12):e0243837. doi:10.1371/journal.pone.0243837
134. Zhang P, Cao Y, Chen H, Zhou B, Hu W, Zhang L. Preparation and evaluation of glycyrrhetinic acid-modified and honokiol-loaded acoustic nanodroplets for targeted tumor imaging and therapy with low-boiling-point phase-change perfluorocarbon. *J Mater Chem B*. 2017;5(29):5845–5853. doi:10.1039/c7tb01215b
135. Calzoni E, Cesaretti A, Polchi A, Di Michele A, Tancini B, Emiliani C. Biocompatible polymer nanoparticles for drug delivery applications in cancer and neurodegenerative disorder therapies. *J Funct Biomater*. 2019;10(1):4. doi:10.3390/jfb10010004
136. Mittal P, Saharan A, Verma R, et al. Dendrimers: a new race of pharmaceutical nanocarriers. *Biomed Res Int*. 2021;2021:8844030. doi:10.1155/2021/8844030
137. Jacob S, Nair AB, Shah J. Emerging role of nanosuspensions in drug delivery systems. *Biomater Res*. 2020;24:3. doi:10.1186/s40824-020-0184-8
138. Zhang W, Shi Y, Abd Shukor S, et al. Phase-shift nanodroplets as an emerging sonoresponsive nanomaterial for imaging and drug delivery applications. *Nanoscale*. 2022;14(8):2943–2965. doi:10.1039/d1nr07882h
139. Ullah R, Shah S, Muhammad Z, et al. *In vitro* and *in vivo* applications of *Euphorbia wallichii* shoot extract-mediated gold nanospheres. *Green Process Synth*. 2021;10(1):101–111. doi:10.1515/gps-2021-0013
140. Shah S, Shah SA, Faisal S, et al. Engineering novel gold nanoparticles using *Sageretia thea* leaf extract and evaluation of their biological activities. *J Nanostructure Chem*. 2022;12:129–140. doi:10.1007/s40097-021-00407-8
141. Abdullah, Rahman Au, Faisal S, Almostafa MM, Younis NS, Yahya G. Multifunctional *spirogyra-hyalina*-mediated barium oxide nanoparticles (BaONPs): synthesis and applications. *Molecules*. 2023;28(17):6364. doi:10.3390/molecules28176364
142. Rizwan M, Faisal S, Tariq MH, Zafar S, Khan A, Ahmad F. *Enterobacter hormaechei*-driven novel biosynthesis of tin oxide nanoparticles and evaluation of their anti-aging, cytotoxic, and enzyme inhibition potential. *ACS Omega*. 2023;8(30):27439–27449. doi:10.1021/acsomega.3c02932
143. Abdullah, Hussain T, Faisal S, et al. Green synthesis and characterization of copper and nickel hybrid nanomaterials: investigation of their biological and photocatalytic potential for the removal of organic crystal violet dye. *J Saudi Chem Soc*. 2022;26(4):101486. doi:10.1016/j.jscs.2022.101486